University of Alberta

Design and Analysis of Complex Composite Structure Subjected to Combined Loading Conditions

by

Rifat Afshana Hossain

A thesis submitted to the Faculty of Graduate Studies and Research
in partial fulfillment of the requirements for the degree of

Master of Science

Department of Mechanical Engineering

Fall 2012

Edmonton, Alberta

ABSTRACT

Axisymmetric fiber-reinforced polymer composite structures such as pressure vessels and piping manufactured by braiding and filament winding are being widely used in different industrial applications where combined loading conditions may be applied. The aim of this study was to determine the distribution of fiber angles along the longitudinal direction of the structure to achieve the best mechanical performance when subjected to combined loadings. A further aim was to develop a suitable failure criterion for structural design. To this end, generalized complex shape mandrel geometries based on variable cross-sections were developed to define mandrel surface equations. Fiber angle variation along the length of an axially symmetric composite structure with variable cross-section was determined considering different ratios of axial loading and internal pressure and by implementing netting analysis design theory. This work was extended to a thorough investigation of failure analysis to provide the critical value of fiber orientation needed to design and analyze complex composite structures subjected to specific loading conditions by incorporating a Tsai-Wu failure criterion.

PREFACE

This thesis is based on work done in the Advanced Composite Materials Engineering and the Biomedical and Composite Materials groups of Mechanical engineering Department, University of Alberta from September 2009 to April 2012 on the design of complex composite structures. The idea of conducting the theoretical study on this topic came forward in order to develop an integrated methodology for the design and analysis of axisymmetric composite structure with variable cross-sections along their length by braiding and filament winding manufacturing processes. This thesis is written in paper format. It consists of five different chapters. In Chapter 1, a brief literature review on the applications and methodologies of designing composite structures by braiding and filament winding technique is presented. At the end of this chapter, the shortcomings of current methods as well as the necessities of the fiber orientation determination and strength analyses are summarized and the objectives of this study to overcome the literature gap are given. In Chapter 2, the design of complex shape mandrels with variable cross-sections and the developed analytical technique to define those characteristic mandrel surface equations are clearly explained. Chapter 3 consists of the methodology for finding the distribution of fiber orientation along the longitudinal direction of the structure subjected to internal pressure and axial loading by implementing netting analysis design theory This work is extended to a thorough investigation of failure analysis to provide the critical value of fiber orientation needed to design and analyze complex composite structures subjected to combined loading conditions by incorporating a Tsai-Wu failure criterion in Chapter 4. Finally, in Chapter 5, the summary of the thesis and the further recommendations are presented to overcome the limitations of this study.

ACKNOWLEDGEMENT

I express heartfelt gratitude to my supervisors Dr. Pierre Mertiny and Dr. Jason Carey for their unique supervision, excellent guidance and considerable patience throughout my MSc. thesis work. I am deeply appreciative for many helpful discussions, mentorship, advising and every other aspect of their work done on my behalf.

I wish to thank Dr. Roger Cheng and Dr. Cagri Ayranci for being part of my defense examination committee members and their constructive comments on this thesis.

It's my pleasure to pay tribute to the funding sources, NSERC and the Mechanical Engineering Department of University of Alberta.

Finally my deepest gratitude goes to my husband Mohammad Al Amin Chowdhuri, for his extraordinary support, commendable encouragement and patience throughout my MSc. research endeavor. Without his cooperation and inspiration, this journey would not be possible for me to come to an end. I also would like to thank my parents and younger brother for keeping their faith on me and providing strong support throughout my life. Today I am here only because of their blessings.

TABLE OF CONTENTS

LIST OF TABLES

LIST OF FIGURES

NOMENCLATURE

A_α	Cross section area of fiber per unit length
E	Fiber Young's Modulus
F	Axial load
F_a	Axial force per unit length
F_h	Hoop force per unit length
H	Heaviside step function
K	Dimensionless variable
R	Radius of the surface path of midsection
a	Axial stress
b	Hoop stress
f	Tsai-Wu failure index
k	Ratio between hoop and axial stress
m	Semi-major axis
n	Semi-minor axis
p	Internal pressure
$r(z)$	Mandrel radius along z direction
t	Dimensionless variable
α	Fiber angle
γ_{ha}	Shear strain
δ	An infinitesimal variable with dimension of length
ε_a	Axial strain
ε_h	Hoop strain
ε_α	Fiber strain
θ	The angle measured from the semi-minor axis.
σ_a	Axial stress
σ_h	Hoop stress
$\sigma_{critical}$	Critical fiber angle
σ_α	Fiber stress

CHAPTER 1

INTRODUCTION

1.1 COMPLEX COMPOSITE STRUCTURES

Composite material structures are widely accepted and successfully employed in the aerospace, marine, automotive, infrastructure and energy industry, where high strength, low weight and chemically resistant components are required. Composite material production versatility provides the opportunity for the design of highly efficient structures [1].

Molded and cast products often require complex shaped structures [2]. Achieving complex shape design requires meeting stiffness and strength requirements best assessed through advanced modeling capable of determining how the individual geometric and structural features interact [3].

An ever increasing range of applications requires complex-shaped composite structures, which in turn necessitates efficient and robust manufacturing methods. The fabrication of complex-shaped composite components may be achieved with established manufacturing techniques such as braiding and filament winding in conjunction with innovative mandrel systems. These two techniques are well suited to produce high performance composite structures [4]. Through adaptation and further development these manufacturing techniques are promising means for producing complex composite structural components at competitive cost compared to other manufacturing techniques, such as dry lay-up, resin transfer molding and pultrusion.

1.2 BRAIDING AND FILAMENT WINDING

Extensive investigations have been carried out for designing and developing the models of complex composite structures by braiding and filament winding. Braiding is a composite material preform manufacturing technique in which a braiding machine deposits continuous, intertwined fiber to create a braided preform before or during the impregnations of fibers with polymeric resin [5]. Filament winding is a manufacturing process where continuous strands of reinforcing fibers are impregnated with resin, then placed onto a rotating mandrel under controlled tension and usually produces cylindrical axisymmetric structures [6]. Munro and Fahim [7] presented the major differences and similarities between braiding and filament winding in terms of design and manufacturing methodology; they found that it was not possible to draw a general conclusion on the better process as selection of the manufacturing technique would be product dependent.

1.2.1 *Complex Structures Design by Braiding*

In the context of braiding complex-shaped structures, Brookstein [8] provided a detailed analysis including the optimum fiber orientation for structural products enabling them to satisfy different load carrying requirements. The analysis was applied to some classical applications of braided structures, where braid reinforcement had replaced conventional materials in many components such as pressure vessels, rods, shafts, plates and structural columns. For example, shafts produced by braiding processes provided stiffness when the fibers were placed along axial direction, and torque transmission reinforcement was provided by $\pm 45^0$ braid. Due to higher specific strength and tailorable mechanical properties, two-dimensional (2D) braiding has been used to manufacture other complex structural components as well. For example, Kobayashi et al. [9] described manufacturing of a braided graphite-epoxy composite truss joint; White [10] focused on manufacturing, testing and cost analysis of Kevlar 49/epoxy blade spar; Casale et al. [11] developed a model for the design and fabrication of sporting equipment, such as a braided bicycle frame using Kevlar/graphite braided hybrid preforms impregnated with epoxy resin. Through a modeling process consisting of altering lamina sequence, Swanek and Carey [12] developed a golf shaft using braided laminas, which would have mass, stiffness and torque comparable to commercially available composite and steel shafts. Moreover, braid reinforced composite materials have been extensively studied for bio-medical applications. Hudgins et al. [13] proposed a prosthetic intervertebral disc to replace a natural disc with a core of elastomeric polymer and a braid reinforced outer shell providing compressive strength to the design. To enhance rigidities of conventional catheters, Carey et al. [14] investigated the application of braided composites for the design of medical catheters.

Several studies have been conducted to design, determine and achieve fiber orientations for different shaped braided preforms [15-19]. Michaeli and Rosenbaum [15] described a computer control system for a braiding machine, which ensured the desired fiber orientation on a symmetric mandrel. However, it was supposed to be difficult to vary the braid angle or to braid parts with varying mandrel diameter. Du and Popper [16] developed a process model considering the micro geometry, such as, braid angle and fiber volume fraction of a conical axi-symmetric braided preform. The authors suggested that a better and uniform braid microstructure can be achieved while braiding over large to small mandrel diameters, and that severe transients in braid angle caused by shape transition can be minimized as well as the uniformity of the braid structure can be improved by reversing the direction of mandrel movement. Kessels and Akkerman [17] presented a fast and efficient model to predict fiber angles for complex bi-axially braided preforms. The model was validated with experiments for two differently shaped mandrels; experimental and numerical results were found to be in good agreement. Liao and Adanur [18] provided a geometric model of braided preforms using the computer aided geometric design technique to represent the fiber path to be braided over the mandrel. According to the authors, the generation of fiber paths on braided preforms based on geometric model often becomes complex whenever the geometry and shape of the desired braided product changes. Another geometrical model was developed by Rawl et al. [19] to provide the fiber orientations of braided preforms with mandrels of different shapes (circular, conical and square prism). They stated that the fiber path on a mandrel is dependent upon the shape of the mandrel. However, the development of characteristic equations for defining the outer surface of mandrels can be a better approach in the case of generating the desired fiber orientation relative to complex mandrel shapes.

1.2.2 *Complex Structures Design by Filament Winding*

In the case of filament winding, due to the high degree of precision with which the reinforcing fibers can be placed onto the surface of the mandrel, the stiffness and strength of a component can be carefully controlled and hence may be tailored to suite specific design requirements [20]. Current applications of filament-wound composites include chemical processing where the outstanding chemical resistance of the material is employed and aerospace and automotive components where high strength-to-weight ratios are important [21]. During the design process, an appropriate set of loads is usually considered and imposed upon the part geometry to verify that it satisfies strength and stiffness requirements. It is a common approach to place the fibers in the direction of maximum stress due to the highly directional nature of continuous fiber reinforcement. In order to predict the mechanical behavior of a composite structure subjected to combined loading, a suitable fiber architecture along the longitudinal direction of the wound structure must be developed.

Filament winding and associated design and analysis work has mostly been conducted for cylindrical axisymmetric composite structures. For example, an experimental investigation was carried out by Mertiny et al. [22] to find the effect of multi-angle filament winding on the strength of tubular composite structures. Beakou and Mohamed [23] pointed out the influence of design variables, such as strengths and loadings on the optimal fiber winding angle of axially loaded cylindrical pressure pipes. It was found that the design of composite structures requires the determination of the fiber orientation based on applied loads and other design constraints. Wild and Vickers [24] presented an analytical procedure based on classical laminated plate theory to assess stresses and deformations of different filament-wound structures under combined loading conditions. In this work also the effects of wind angle variation through the cylindrical wall was assessed. To date, filament winding has mostly been restricted to tubular and other relatively simple axisymmetric shapes, which constitute a significant limitation on the range of items that can be fabricated [7]. Recently, researchers have attempted to extend the filament winding technique to more complex shape structures for specific design requirements. For example, to effectively utilize the filament winding capabilities, Mazumdar and Hoa [25-27] presented geometry-based approaches to generate the desired fiber distribution on cylindrical, axisymmetric as well as complex-shaped mandrels. According to the authors, winding on non-cylindrical mandrels with curved cross-sections was not addressed in their work. Carvalho et al. [28] developed a methodology with an integrated numerical (finite element) analysis for the design of filament-wound parts. The test case of a conical filament-wound part was presented for a simplified torsional loading condition. This methodology included the determination of ideal fiber orientations using finite element analysis, generation of feasible fiber paths, determination of the final lay-up sequence, and an analysis to adapt the final lay-up to meet strength and stiffness requirements. The proposed methodology produced a final optimum fiber orientation after a few iterations. For more demanding part configurations it was suggested to proceed with additional iterations. Several works were also dedicated to winding the dome geometry of non-spherical pressure vessels. In this context Jones et al. [29] conducted a geometric analysis to derive a winding technique for improved layup efficiency and mechanical performance. It was recommended to develop an accurate wind angle distribution to precisely predict the behavior of the wound dome part. Teng et al. [30] attempted to optimize the design of dome shaped composite vessels to withstand a maximum internal pressure. The design variables used to optimize the dome geometry were the winding angle and the ratio of major and minor axes of the dome part. Park et al. [31] studied the behavior of the dome part of pressure vessel subjected to internal pressure, calculated the wind angle variation at the dome geometry, and also quantified the fiber angle change through the thickness direction.

1.2.3 *Implementation of Design Criterion*

Braided and filament-wound structures are frequently used in applications in which combinations of internal/external pressure, bending, torsion and axial loading may be present. To devise a suitable fiber architecture it is generally necessary to employ an approach which implements a design or failure criterion. Damage in cylindrical composite structures under combined loading is a complex phenomenon involving a variety of failure mechanisms [32]. Understanding the failure process and the development of reliable failure criteria is an essential prerequisite for efficient analysis and design. There are various methods for analyzing stresses and strains associated with combined loading conditions, including netting analysis [24], orthotropic analysis [33], and finite element analysis [28, 34]. Netting analysis is a simplified yet expedient approach for the design of fiber-composite structures, providing the relationship between the fiber orientations and the loading conditions applied to the structures. Under the assumption of plane stress, orthotropic analysis may be used to predict the behavior of a composite structure under loading and thus determine fiber orientations. Finite element analysis further allows for modeling the composite as a detailed layered laminate and defining optimal ply stacking [28]. The lay-up may thus be modified to achieve strength and stiffness requirements.

In order to fulfill the design requirements for the complex structures considered herein, it is essential to suitably adapt some of the aforementioned design and failure criteria. At a certain applied load, composite failure starts within the most stressed lamina in a laminate, followed by the sequence of next-to-be-most-stressed lamina leading eventual to ultimate failure when all the layers have failed. To this end, a lamina criterion is usually assumed along with employing lamina input and lamination theory to evaluate stresses and strains in the various plies. For example in [35], using laminate theory and netting analysis, theoretical failure envelopes were obtained and contrasted to experiments carried out for ±55° angle-ply pipes subjected to biaxial loading of internal pressure and axial force. Similarly, experimental data were gathered in [36] to show the influence of fiber orientation on the deformation and strength of filament-wound glass fiber reinforced tubes subjected to a variety of uniaxial and biaxial membrane stresses. The experimental results demonstrated the variation of failure strengths of glass fiber reinforced epoxy tubes with ±45°, ±55° and ±75° fiber architectures for different combinations of internal pressure and axial load. It was observed that netting analysis reasonably predicted ultimate strength, noting that it is only applicable to one specific hoop-to-axial stress ratio for each layup configuration as it cannot be used to predict resin-related contributions to mechanical performance. In the same manner, material non-linearities cannot be captured. Notably, netting analysis did not necessarily predict the maximum measured biaxial stress state for the samples tested. Apart from netting analysis, in order to analyze the stresses and strains in a multi-layer cylindrical shell (orthotropic analysis), Lekhnitskii [33] developed a solution for the problem of plane stress in the shell which is cylindrically orthotropic and subjected to internal and external pressures. In the case of filament-wound composite pressure vessels with dome shaped parts the design of the dome is a major part of the design as it tends to be the location of failure. This is due to the fact that the dome region undergoes the highest stress levels, making it the most critical locations from the viewpoint of structural failure. For example, Hofeditz [37] discussed the use of netting theory and orthotropic analysis methods to solve design problems involving dome shapes; Hojjati et al. [38] designed dome contours based on the theory of orthotropic plates; Lin and Hwang [39] established design techniques for dome shapes based on composite failure criteria and for determining dome contours based on the theory of orthotropic analysis. Finite element analysis may be considered as alternative approach for the design of fiber-composite layered laminate. For example, Neto et al. [34] investigated the behavior under burst pressure testing of a pressure vessel liner, where the design and failure prediction of the composite laminate polymeric liner was conducted using finite element analysis. The carbon/epoxy laminate was built using angle-ply layers. Six different preliminary finite element analysis simulations were carried out using sub-laminates with layers oriented at ±10°, ±20°, ±30°, ±40°, ±50° and ±60°. According to these simulations the ±40° laminate showed the best performance in terms of strength.

In addition to the abovementioned design criteria, further research work has focused on the failure analysis of laminated composite structures over the years. Several approaches have been proposed, including non-linear viscoplastic constitutive modeling, fracture mechanics, damage mechanics and macroscopic (global) failure criteria [40]. Although many investigations have formulated composite failure criteria, phenomenological failure criteria are still the predominant choice for the design in industrial applications [41]. Such failure theories are based on the local stresses or strains in a lamina. For an angle lamina, global stresses/strains first need to be transformed into a local fiber-based coordinate system. Then a judgment can be made whether the lamina will fail or not. The most common failure criteria can be grouped into two different classes: linear and quadratic. To be more specific, there are three major types of engineering failure criteria for unidirectional composite materials: maximum stress criterion, maximum strain criterion, and quadratic interaction criteria, such as the Tsai-Hill and Tsai-Wu failure theories [42].

For design and analysis of composite structures, the linear and quadratic failure criteria have been employed in different industrial applications under combined loading conditions. For example, Eckold et al. [43] described a theoretical approach to the prediction of failure envelopes for filament-wound materials under biaxial loading using a maximum stress failure criterion that provided the mode of failure. Good correlation was found with experimental results. However the employed failure criterion was found to be less accurate than a distortional energy failure approach for assessing the strength of the material under axial load and internal pressure with reasonable accuracy. Gargiulo et al. [44] predicted the failure behavior of composite tubes where internal or external pressure and axial loads were applied simultaneously to produce a variety of biaxial stress conditions. The authors examined the effect of the winding angle of fiber reinforcements on the failure loads and provided numerical and experimental data on the strength of the filament wound pipes. Finite element analysis was applied to the problem using Tsai-Wu failure criterion in order to predict the specimen failure for a comparison with experimental results. Onder et al. [40] investigated the burst pressure of filament-wound composite pressure vessels under alternating pure internal pressure and experimental approaches were employed to verify the optimum winding angles. The Tsai-Wu failure criterion and the maximum stress theory were applied and contrasted with burst failure pressures of the vessels. However, failure analyzed was only based on pure internal pressure rather than a wide range of loading conditions. Srikanth and Rao [45] presented the experimental strength and stiffness properties of both braided and filament-wound carbon fiber reinforced polymer composites, fabricated with varied fiber orientations (2° to 88°). The properties of braided and filament-wound composites decreased with increased fiber orientation. Also, filament-wound composite exhibited initial higher modulus and strength values compared to braided composites (up to 30° fiber orientation). This difference vanished for larger angles in both braided and filament wound composites. Their work also showed good correlations with predictions made by conventional modeling approaches, i.e. classical laminate theory and the Tsai-Wu criterion.

1.3 SCOPE OF THE STUDY

From the above review it becomes apparent that a number of research articles are available in the technical literatures that recognize the growing need and potential application of braided and filament-wound composites. However, literature providing methodologies for braiding and filament winding over complex-shaped mandrels to design and analyze complex composite structures subjected to combined loading conditions is limited. Even though research work on braiding of complex structures is available to some extent, the same cannot be said for complex structures made by filament winding. Most of the available modeling predicts an ideal fiber orientation to satisfy strength and stiffness requirements for conventional filament-wound structures (i.e. cylindrical piping and pressure vessels) or dome-shaped vessels under specific loading conditions. No models were found for the design of complex-shaped structures with variable cross-section along the mandrel length under combined loadings to determine the fiber orientation and its variation along the longitudinal direction. Hence, providing an expedient technique using a suitable design theory such as netting analysis for computing the fiber angle variation along the length of an axially symmetric part with variable cross-section subjected to different ratios of axial loading and internal pressure is considered an innovative contribution.

As mentioned above, through netting analysis only a single fiber angle can be found for a fixed ratio between hoop and axial stresses. Such a fiber angle would not necessarily comply with variable loading conditions composed of e.g.

internal pressure and axial traction. Thus, the design process must incorporate the examination of properties such as strength for stress ratios that deviate from initial netting analysis results. For this purpose a suitable quadratic failure theory may be implemented providing an enhanced and safer design approach. The present study thus presents an innovative expedient methodology for determining the fiber angle distribution for given complex part geometries and loading conditions by initially incorporating netting analysis theory. The methodology is then extended by implementing Tsai-Wu failure analysis in order to provide critical fiber orientations needed to assess the structure performance and strength for combined loading conditions. This study is seen as the foundation for a design framework yielding braiding or filament winding manufacturing parameters for complex-shaped structures subjected to variable loading conditions.

1.4 THESIS OBJECTIVES

The objectives of research work described in this thesis are as follows:

1. Design of axially symmetric complex-shaped mandrels with varying dimensions and cross-sections along their length, and development of an analytical technique for defining the characteristic complex-shaped mandrel surface equations.

2. Determination of the fiber angle variation along the length of the composite structures with variable cross-section considering different ratios of axial loading and internal pressure. As an initial step, netting analysis design theory is implemented, providing the relationship between the fiber orientation and a given loading condition applied to the structure.

3. Development of a methodology based on the Tsai-Wu failure criterion to assess feasible fiber angles for variable loadings. The aim is to obtain critical fiber angles for the variation of axial and/or hoop stress. The theoretical investigation will consider two different material systems, i.e. E-glass fiber/epoxy and carbon fiber/epoxy.

1.5 REFERENCES

1. Gibson, F. R., 2010, “A review of recent research on mechanics of multifunctional composite materials and structures”, Composite Structures, 92, 2793–2810.

2. Farin, G., 1990 “Curves and Surfaces for Computer Aided Geometric Design: A Practical Guide”, Academic Press Inc., Boston, MA.

3. http://mfgcommunity.autodesk.com/files/blog/amy/Complex.pdf (accessed January 6, 2011).

4. Kamiya, R., Cheeseman, B. A., Chou, T.W., 2000, “Some recent advances in the fabrication and design of three-dimensional textile preforms: a review”, Composites Science and Technology, 60, 33-47.

5. Ayranci, C., Carey, J., 2008, “2-D braided composites: a review for stiffness critical applications”, Composite Structures, 85(1), 43-58.

6. Carvalho, J. D., Lossie, M., Vandepitte , D., Van Brussel, H., 1995, “Optimization of filament-wound parts based on non-geodesic winding”, Composites Manufacturing, 6, 79-84.

7. Munro, M., Fahim. A., 1995, “Comparison of helical filament winding and 2D braiding of fiber reinforced polymeric components”. Materials Manufacturing Process, 10(1), 37–46.

8. Brookstein,D. 1988, “Structural applications of advanced braided composites”, Proceedings SPE/APC’88. Advanced polymer composites for structural applications, Los Angeles, CA, 415–424.

9. Kobayashi, H., Nakama, N., Maekawa, Z., Hamada, H., Fujita, A., Uozumi, T., 1992, “Fabrication and mechanical properties of braided composite truss joint”, 37th International SAMPE symposium and exhibition, Anaheim, CA, 1089–1103.

10. White, M.L., 1982, “Tubular braided composite main rotor blade spar”, Journal of the American Helicopter Society, 4, 45–48.

11. Casale, N., Bristow, D., Pastore, C.M., 1991, “Design and fabrication of a braided composite monocoque bicycle frame”, High-Tech fibrous materials: ACS symposium series, 457, 90–101.

12. Swanek, D.S., Carey, J., 2007, “Braided composite materials for the production of lightweight, high rigidity golf shafts”, Sports Engineering, 10 (4), 195-208.

13. Hudgins, R.G., Muzzy, J.D., 1998, “Analytical stress model for a composite prosthetic intervertebral disc”, Polymer Composites, 19(6), 837–845.

14. Carey, J., Fahim, A., Munro, M., 2004, “Design of braided composite cardiovascular catheters based on required axial, flexural, and torsional rigidities”, Journal of Biomedical Materials Research Part B: Applied Biomaterials, 70(1), 73–81.

15. Michaeli, W., Rosenbaum, U., 1989, "Structural braiding of complex-shaped FRP parts: A new approach for higher productivity," 34th International SAMPE Symposium, Covina, CA, 1834-1842.

16. Du, G.W., Popper, P. 1994, "Analysis of a Circular Braiding Process for Complex Shapes", Journal of the Textile Institute, 85(3), 316–337.

17. Kessels, J.F.A., Akkerman, R., 2001, "Prediction of the yarn trajectories on complex braided preforms," Composites A, 33 (8), 1073–1081.

18. Liao, T., Adanur, S., 2000, "3D Structural Simulation of Tubular Braided Fabrics for Net-Shape Composites," Textile Research Journal, 70, 297-303.

19. Rawl, A., Potluri, P., Steele, C., 2005, "Geometrical Modeling of the Yarn Paths in Three-dimensional Braided Structures", Journal of Industrial Textiles, 34(2), 115-135.

20. Menges, G., Wodicka, R., Barkling, H.L., 1978, "Non-geodesic winding on a surface of revolution", 33rd Annual Technical Conference, Reinforced Plastics/ Composites Institute, New York.

21. Mazumder, S. K. and Hoa, S.V. 1992, "Filament winding on tapered axisymmetric and non-axisymmetric composite components", 13th International SAMPE Conference, Covina, CA.

22. Mertiny, P., Ellyin, F., Hothan, A., 2004, "An experimental investigation on the effect of multi-angle filament winding on the strength of tubular composite structures", Composites Science and Technology, 64, 1-9.

23. Beakou, A., Mohamed,A., 2001, “Influence of variable scattering on the optimum winding angle of cylindrical laminated composites”, Composite Structures, 53 (3) , 287-293.

24. Wild, P.M., Vickers, C.W., 1997, “Analysis of filament-wound cylindrical shells under combined centrifugal, pressure and axial loading”, Composites A, 28 (1), 47-55.

25. Mazumdar, S.K., Hoa, S.V., 1995, “Analytical model for low cost manufacturing of composites components by filament winding, Part1: direct kinematics”, Journal of Composite Materials, 29, 1515-1541.

26. Mazumder, S. K., Hoa, S.V., 1991, ”On the kinematics of filament winding on non-axisymmetric cylindrical mandrels, Part 1: A generalized model”, Composites Manufacturing, 2, 23-30.

27. Mazumder, S. K., Hoa, S.V., 1992, “Filament winding on tapered axisymmetric and non-axisymmetric composite components”, 13th International SAMPE Conference, Covina, CA.

28. Carvalho, J.D., Lossie, M., Vandepitte, D., Van Brussel, H., 1995, “Optimization of filament-wound parts based on non-geodesic winding”, Composites Manufacturing, 6, 79-84.

29. Jones, D.T., Jones, I.A., Middleton V., 1996, “Improving composite lay up for non-spherical filament wound pressure vessels”, Composites A, 27, 311-317.

30. Teng, T.L., Yu, C.M., Wu, Y.Y., 2005, "Optimal design of filament-wound composite pressure vessels", Mechanics of Composite Materials, 41 (4), 333-340.

31. Park, J., Hong, C., Kim, C., Kim, C., 2002, "Analysis of filament wound composite structures considering the change of winding angles through the thickness direction", Composites Structures, 55, 63-71.

32. Hull, D., 1981, "An Introduction to Composite Materials", Cambridge University Press, London, United Kingdom.

33. Lekhnitskii, S.G., 1968, "Anisotropic Plates", Gordon and Breach Science Publishers, London, United Kingdom.

34. Barboza Neto, E.S., Chludzinski, M., Roese, P.B., Fonseca, J.S.O., Amico, S.C., Ferreira, C.A., 2011, "Experimental and numerical analysis of a LLDPE/HDPE liner for a composite pressure vessel", Polymer Testing, 30, 693–700.

35. Soden, P. D., Kitching, R., Tse, P.C., 1989, "Experimental failure stresses for $\pm 55^{\circ}$ filament wound glass fiber reinforced plastic tubes under biaxial loads", Composites, 20 (2), 125-135.

36. Soden, P.D., Kitching, R., Tse, P.C., Tsavalas, Y., Hinton, M.J., 1993, "Influence of filament winding angle on the strength and deformation of filament-wound composite tubes subjected to uniaxial and biaxial loads", Composites Science and Technology, 46, 363-378.

37. Hofeditz, J.T., 1963, "Structural design considerations for glass pressure vessels", 18th Annual Meeting of the Reinforced Plastics Division.

38. Hojjati, M., Safavi, A.V., Hoa, S.V., 1995, "Design of dome for polymeric composite pressure vessels", Composite Engineering, 5(1), 51-59.

39. Lin, Y.C., Hwang, W.C., 1995, "Design of dome contour for filament wound rocket motor cases", Transactions of the Aeronautical and Astronautical Society of the Republic of China, 27(1), 61-70.

40. Onder, A., Sayman, O., Dogan, T., Tarakcioglu, N., 2009, "Burst failure load of composite pressure vessels", Composites Structures, 89 (1), 159-166.

41. Roylance, D.K., 1976, "Netting analysis for filament wound pressure vessels", Technical Report 76-3, Composites Division, Army Materials and Mechanics Research Center, Watertown, MA.

42. Kaw, A. K., 1997, "Mechanics of composite materials", CRC Press, NY.

43. Eckold, G.C., Leadbetter, D., Soden, P.D., Griggs, P.R., 1978, " Lamination theory in the prediction of failure envelopes for filament wound materials subjected to biaxial loading," Composites 9(4), 243-246.

44. Gargiulo, C., Marchetti, M., Rizzo, A., 1996, "Prediction of failure envelopes of composite tubes subjected to biaxial loadings," Acta Astronautica 39(5), 355-368.

45. Srikanth, L., Rao, R. M.V.G. K., 2011. "Concurrent studies on braided and filament wound carbon fiber composites - a comparative appraisal", Journal of reinforced plastics & composites, 30 (16), 1359-1365.

CHAPTER 2: COMPLEX-SHAPED MANDREL MODELING FOR BRAIDING AND FILAMENT-WINDING

A version of this chapter was published as:

Hossain, R., Carey, J. P., and Mertiny, P., 2011, "Complex-shaped mandrel modeling for braiding and filament-winding," 23rd Canadian Congress of Applied Mechanics, Vancouver, June 6-9, paper no: 124.

CHAPTER 2

2.1 INTRODUCTION

Complex shapes are often found in molded and cast consumer products and parts that possess complicated draft surfaces, smooth surface continuity between part faces, and surface geometries that are based on splines rather than line and arc profiles [1]. Growing demand exists for more complex yet aesthetically pleasing designs in several industries [2]. The need for structural components with high specific stiffness and strength is increasing rapidly in several fields as well, which drives the development of efficient and robust methods for the manufacturing of fiber-reinforced polymer composites. Polymer composites made by braiding and filament winding have significant potential for improving the performance of complex-shaped structural components [3]**.** Both of these fabrication methods can be highly automated and thus produce low-cost and reliable composite structural components [4]. Through adaptation and further development, braiding and filament winding have become promising methods for producing complex structural components.

Several studies were carried out for developing models of braided and filament-wound complex-shaped structures [5-15]. Braiding is a versatile textile process experiencing a resurgence because of its diverse applications [4] and new opportunities in near net shape manufacturing of structures with high damage resistance. A detailed method for geometrically describing the braided preforms was reported by Wang and Wang [5, 6] who determined that the geometry is characterized by a set of physical parameters. Values for these parameters can be determined by measuring certain physical features on the preform exterior. However a general mandrel shape design has not been given preference in this study which limits an increased flexibility for the design of different braided preforms. The same authors [7] also explored a concept that links the initial braid design to the final composite properties using a braided preform with tubular cross-section. Moreover, Wang and Wang [8] developed a general methodology for determining the permissible fiber orientation of two preforms that have similar yarn structures but with different shapes such as rectangular and curvilinear cross-sections. Rawl et al. [9] reported that the fiber path on a mandrel is dependent upon the shape of the mandrel, e.g. for a circular shape the path will be in the form of a helix whereas for a cubical body the path will be in the form of straight lines. They also presented mathematical models to generate fiber orientations for mandrels of different shapes (circular, conical and square prism). However it was recommended that development of characteristic equations for such mandrel shapes would expedite the process of generating desired fiber orientation relative to mandrel shape. Liao and Adanur [10] developed another geometric model of braided preforms using a computer aided geometric design technique. At first the way to represent the fiber path to be braided over the mandrel is presented and finally some applications of the modeling on net-shape structures were demonstrated. Clearly, there was a need for an accurate data base on the physical properties of braided composites and the derivations of respective mandrel surface equations, reported by the authors, which was indicated as their future work.

Filament winding has been used extensively for the manufacturing of cylindrical axisymmetric structures. For example, an experimental investigation was carried out by Mertiny et al. [11] to find the effect of multi-angle filament winding on the strength of tubular composite structures. To effectively utilize the capabilities of filament winding, some geometry-based approaches have been presented by Mazumdar and Hoa [12] to determine the desired fiber distribution along a cylindrical axisymmetric mandrel surface. During the past two decades, several authors [13-15] have performed detailed analyses utilizing analytical and experimental approaches to filament winding on the design and fabrication of dome shaped pressure vessel. This is due to the fact that the dome regions undergo the highest stress levels and are the most critical locations from the viewpoint of structural failure [15]. Teng et al. [14] focused on the application of dome shape pressure vessel design to provide optimum fiber angle under pure internal pressure. However further development to this procedure should be included in this study for the selection of feasible wind angles along with application of other loading conditions.

The above literature review shows that different methodologies are available for predicting the fiber orientation for mostly rather simple braided and filament-wound preforms. It is proposed to use derivatives of these models to extend them to more complex-shaped mandrels. The objective of part of this research project is to design complex-shaped mandrels with varying dimensions and cross-sections along their length and develop models for the design of braided and filament-wound preforms subjected to loading conditions. This paper focuses on the development of generalized complex shape mandrel geometries based on different cross-section shapes and the development of an analytical technique for defining complex-shaped mandrel surface equations.

2.2 USE OF MANDREL SURFACE EQUATIONS FOR DETERMINING FIBER ORIENTATION

As mentioned above, this research aims at developing complex-shaped composite structures that can be manufactured using braiding and filament winding processes. This task can be divided into a combination of several processes, i.e. the design of a mandrel shape, the analytical description of the mandrel surface, and the determination of fiber orientations based on material properties and loading conditions that best satisfy design requirements such as strength and stiffness. Simulating the structure under applied loadings allows for deriving ideal fiber orientations for fiber path planning. In many cases the ideal fiber orientation is in the resultant force direction. To obtain accurate fiber placements, fibers must not slip on the surface during winding/braiding. Also, depending on the geometry of the structure, problems of fiber bridging may occur [12]. Fiber path planning may involve geodesic fiber paths (shortest distance between two points on a mandrel surface), which can be generated considering the start winding/braid angle at the origin. During winding this angle may then be varied to achieve a feasible fiber path for a given mandrel geometry [14].

It is apparent that the mandrel shape plays an important role in determining fiber orientation. Generally the orientation along the mandrel surface cannot be obtained directly for complex-shaped mandrels. Modeling of relevant mandrel shapes and determining characteristic mandrel surface equations is therefore an important step towards generating variation of fiber orientation along the mandrel surface subjected to different loading conditions.

2.3 DEFINITION OF DIFFERENT COMPLEX-SHAPED MANDREL GEOMETRIES

Here, mandrel geometries were chosen to represent common practical shapes of complex composite structures. The geometry and coordinate system (Cartesian shown) of the various mandrel models are defined in Figure 2.1.

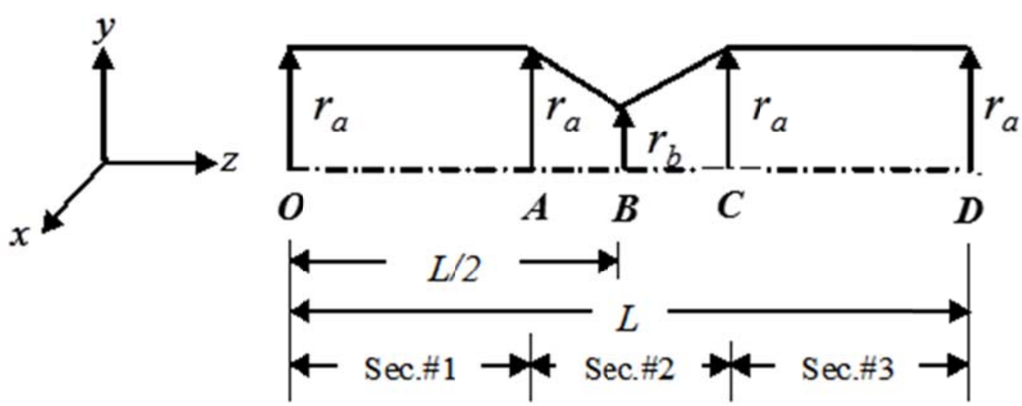

Figure 2.1: Generalized mandrel shape.

The mandrel geometry was divided into three sections along its length in z-direction. These sections have lengths $(z_a - z_0)$, $(z_c - z_a)$ and $(z_d - z_c)$ respectively. For the first section, a uniform characteristic dimension r_a was defined, which in the present case is equal to the dimension of the third section. In the second section the cross-section was assumed to be convergent-divergent along the section length. The dimension at point B along the mandrel length was defined as r_b. In the present analysis four different cases were considered. These are shown as solid models in Figure 2.2, i.e. mandrels with cross-section shapes that are circular with either abruptly changing section slopes or smoothly changing slope along the middle section, ellipsoid and rectangular are shown in Figures 2.2(a) to 2.2(d) respectively. The solid models, which are suitable for fabricating physical mandrels, were produced using SolidWorks CAD software (Concord, Massachusetts, USA).

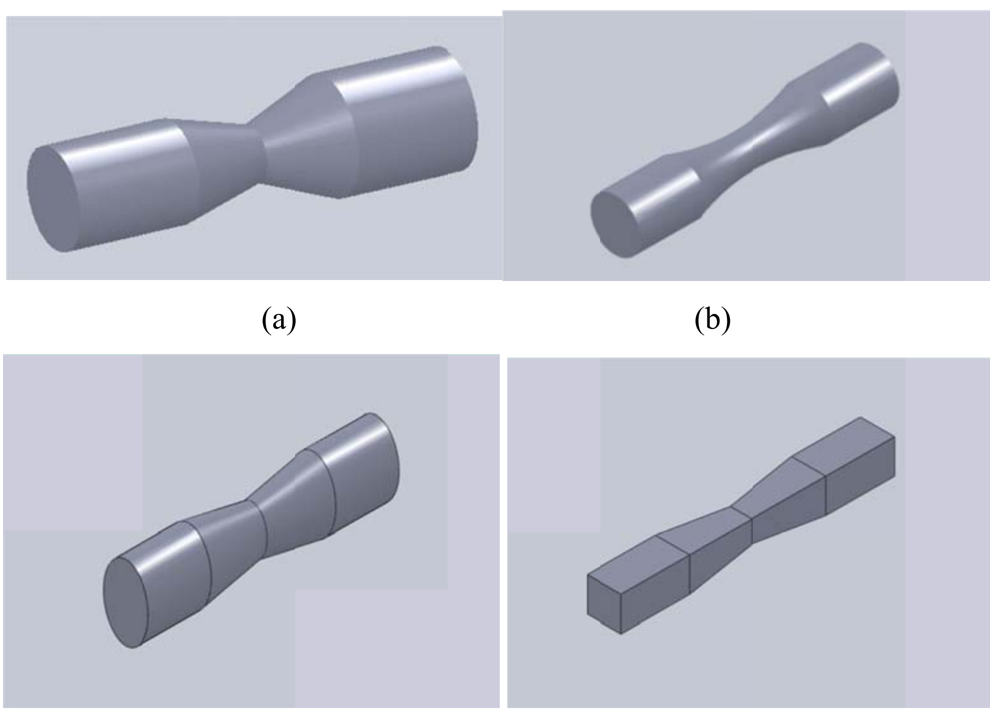

(a) (b)

(c) (d)

Figure 2.2: Mandrel shapes with different cross-sections: (a) circular (abruptly changing slopes), (b) circular (smoothly changing slope), (c) ellipsoid, (d) rectangular.

2.4 ANALYTICAL MODEL DEFINING MANDREL SURFACE

The surface of an axisymmetric mandrel having similar cross-sections at both ends, such as cones, ellipses, parabola and spheroids, can be generated by revolving a curve about an axis [12] and is represented by,

$$r = f(z) \tag{1}$$

where r is the radial distance of a point on the mandrel surface from the central axis and z is the axis of revolution. Note that a description using cylindrical coordinates is conducive to braiding and filament winding where machine motions are defined in the same manner. Similarly, ruled surfaces cover a wide range of mandrel shapes, such as axisymmetric, non-axisymmetric, cylindrical and non-cylindrical geometries [1].

An effective way for determining the relative position of the mandrel and delivery point for a desired fiber lay-down path is representing the total mandrel surface as a combination of several shapes. For example, a ruled surface mandrel can be approximated as a number of trapezoidal faces, whereas an axisymmetric mandrel can be approximated by truncated cones [12]. Such approximations reduce the analytical model complexity.

Circular cross-section throughout mandrel length

For the mandrel shapes considered herein, surface equations were developed for each segment, and finally, combining each segment provided the global equation set. For example, if the cross-section is circular throughout the mandrel length, i.e. case (a) in Figure 2.2, the characteristic equation of the mandrel surface is:

$$r(z) = r_a \times H(t) + [K \times r_a + (1-K)r_b] \times H(-t) \tag{2}$$

where $K = |z_b - z|(z_b - z_a)^{-1}$ a dimensionless variable is used to characterize the convergent-divergent section; $t = (z_{a+\delta} - z)(z_{c-\delta} - z)^{-1}$ is another dimensionless variable used with the Heaviside step function H; and δ is an infinitesimal variable with dimension of length.

From Eq. (2), for the first section in Figure 2, i.e. $0 \le z \le z_a$, the value of $r(z)$ is r_a when $t > 0$. Similarly for the third section, $z_c \le z \le L$, the value of $r(z)$ is r_a when $t > 0$. But for the second section, $z_a \le z \le z_b$ and $z_b \le z \le z_c$, the value of $r(z)$, when $t < 0$, is defined by the term $[K \times r_a + (1-K)r_b]$. At point B, the dimension is r_b, and elsewhere the dimension is determined by K. It could be mentioned here that $z_b - z_a$ and $z_c - z_b$ were taken to be equal in length and none of the quantities can be negative.

The equation for circular mandrel cross-section shapes with smoothly changing slope along the midsection (Figure 2.2 (b)) is given by:

$$r(z) = r_a \times H(t) + \left[r_a + \sqrt{R^2 - (z_b - z_a)^2} - \sqrt{R^2 - (z_b - z)^2} \right] \times H(-t) \tag{3}$$

where R is the radius of the surface path of midsection and can be expressed by the following equation:

$$R = (1/2)\left[(r_a - r_b) - \frac{(z_b - z_a)^2}{(r_b - r_a)} \right]$$

The difference between Eq.(2) and (3) lies in the second section. In Eq.(2) the change from the first to second section or from the second to third section is sudden and the surface path within the second section is linear, whereas for Eq.(3) the above changes are continuous and the surface path is arc-shaped with radius *R*.

Ellipsoidal cross-section throughout mandrel length

The characteristic dimension of an ellipsoid cross-section is defined by *r(z,θ)*. So for ellipsoid mandrel (Figure 2.2 (c)), θ is the parameter to be considered along with z to find the surface equation as the following:

$$r(z,\theta) = r_a(\theta) \times H(t) + [K \times r_a(\theta) + (1-K) r_b(\theta)] \times H(-t) \quad (4)$$

where, $r_a(\theta) = \dfrac{m_a n_a}{\sqrt{n_a^2 \cos^2\theta + m_a^2 \sin^2\theta}}$ and

$$r_b(\theta) = \frac{m_b n_b}{\sqrt{n_b^2 \cos^2\theta + m_b^2 \sin^2\theta}}$$

In Eq.(4), *m* and *n* are semi-major and semi-minor axes, respectively. Here, *m* and *n* correspond with the *y* and *x* axes; θ is the angle measured from the semi-minor axis.

Rectangular cross-section throughout mandrel length

For quadrilateral cross-section shapes (e.g. rectangle) a Cartesian representation was defined first, i.e. $x(z)$ and $y(z)$ for rectangles. Then an appropriate transformation should be provided for cylindrical coordinates. Using a cylindrical coordinate system (theta and z) seems conducive to our problem, for both braiding and filament winding, where the mandrel is rotating with theta and the fiber path is traveling along the mandrel z-position.

$$x(z) = x_a \times H(t) + \left[K \times x_a + (1-K)x_b\right] \times H(-t) \tag{5a}$$

$$y(z) = y_a \times H(t) + \left[K \times y_a + (1-K)y_b\right] \times H(-t) \tag{5b}$$

The following expression is used to transform above equations for rectangular cross-section shapes ((Figure 2.2 (d)) into cylindrical coordinates:

$$r(z,\theta) = \left| \frac{x}{\cos(\theta)} H(t_1) + \frac{y}{\sin(\theta)} H(-t_1) \right| \tag{6}$$

where, $t_1 = \left[\dfrac{\theta - \arctan(yx^{-1}) + \delta}{\pi - \theta - \arctan(yx^{-1}) - \delta} \right] \left[\dfrac{\theta - \pi - \arctan(yx^{-1}) + \delta}{2\pi - \theta - \arctan(yx^{-1}) - \delta} \right]$

Point clouds shown in Figures 2.3(a) to 2.3(d) correspond to Eqs.(2) to (6); parameters were chosen arbitrarily. Graphs were produced using MathWorks MATLAB numerical computing software (Natick, MA).

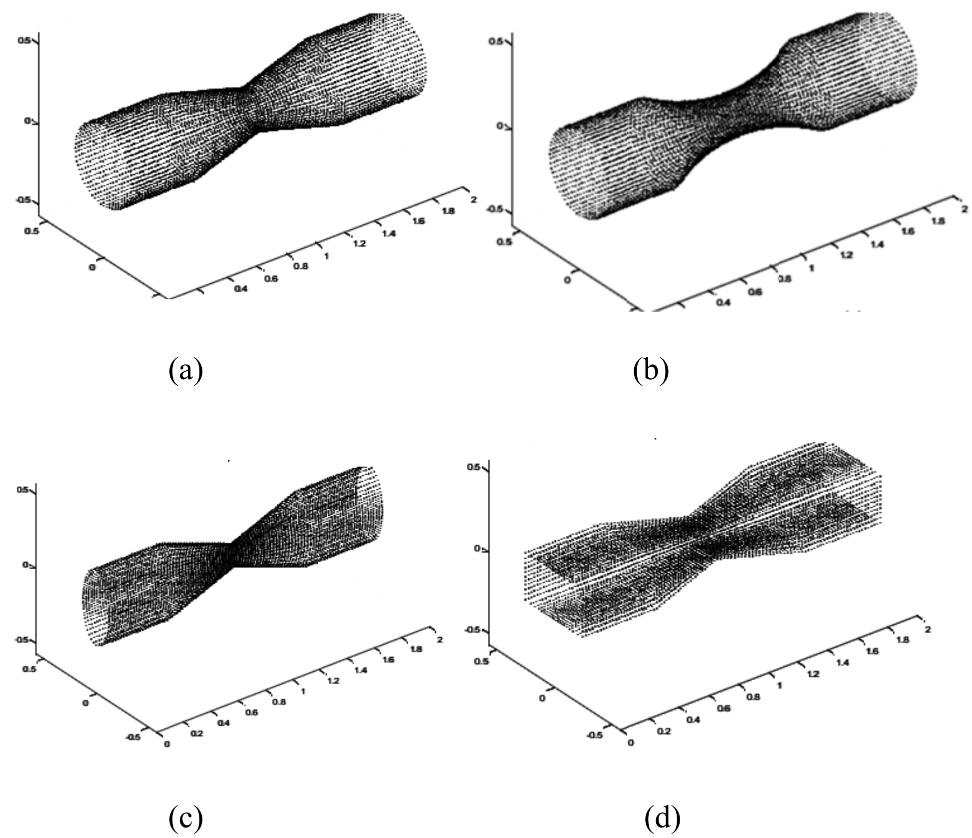

Figure 2.3: Point cloud representing characteristic equation for mandrel shape with different cross-sections, (a) circular (abruptly changing slopes), (b) circular (smoothly changing slope), (c) ellipsoid, (d) rectangular.

2.5 CONCLUSIONS

An analytical technique that represents different complex-shaped mandrels for braiding and filament winding was developed by defining appropriate mandrel surface equations. Four sample cases of mandrels with different cross-section shapes were presented. Based on the characteristic surface equations, different mandrel shapes can be defined, which will be used determine the desired fiber orientation of any complex mandrel shape using braiding or filament winding. Work presented herein is considered a first step towards developing an expedient method for fabricating complex-shaped braided or filament-wound structures. In future work, an analytical model will be developed that provides the variation of fiber orientation along the length of mandrel surfaces with variable cross-sections under combined loading conditions.

2.6 REFERENCES

1. Farin, G., 1993, "Curves and Surfaces for Computer Aided Geometric Design: A Practical Guide", Academic Press Inc., Boston, MA, 3rd Edition.
2. http://mfgcommunity.autodesk.com/files/blog/amy/Complex.pdf (accessed January 6, 2011).
3. Kamiya, R., Cheeseman, B. A., Chou, T.W., 2000, "Some recent advances in the fabrication and design of three-dimensional textile preforms: a review", Composites Science and Technology, 60, 33-47.
4. Ayranci, C., Carey, J., 2008, "2-D braided composites: a review for stiffness critical applications", Composite Structures, 85(1), 43-58.
5. Wang, Y. Q., Wang, A. S. D., 1994, "On the topological yarn structure in 3-D rectangular and tubular braided preforms", Composites Science and Technology, 51, 575-586.
6. Wang, Y.Q., Wang, A. S. D., 1995, "Microstructure property relationships in three-dimensionally braided fiber composites", Composites Science and Technology, 53, 213-222.
7. Wang, Y. Q., Wang, A. S. D., 1997, "Spatial Distribution of Yarns and Mechanical Properties in 3D Braided Tubular Composites", Applied Composite Materials, 4, 121-132.
8. Wang, Y. Q., Wang, A. S. D., 1995, "Geometric Mapping of Yarn Structures due to Shape change in 3-D Braided Composites", Composites Science and Technology, 54, 359-370.

9. Rawl, A., Potluri, P., Steele, C., 2005, "Geometrical Modeling of the Yarn Paths in Three-dimensional Braided Structures", Journal of Industrial Textiles, 34(2), 115-135.

10. Liao, T., Adanur, S., 2000, "3D Structural Simulation of Tubular Braided Fabrics for Net-Shape Composites", Textile Research Journal, 70, 297-.

11. Mertiny, P., Ellyin, F., Hothan, A., 2004, "An experimental investigation on the effect of multi-angle filament winding on the strength of tubular composite structures", Composites Science and Technology, 64, 1-9.

12. Mazumdar, S.K., Hoa, S.V., 1995, "Analytical model for low cost manufacturing of composites components by filament winding, part1: direct kinematics", Journal of Composite Materials, 29(11), 1515-1541.

13. Wild, P.M., Vickers, C.W., 1997, "Analysis of filament-wound cylindrical shells under combined centrifugal, pressure and axial loading", Composites: A, 28, 47-55.

14. Teng, T.L., Yu, C.M., Wu, Y.Y., 2005, "Optimal design of filament-wound composite pressure vessels", Mechanics of Composite Materials, 41 (4), 333-340.

15. Carvalho, J. D., Lossie, M., Vandepitte, D., Van Brussel, H., 1995, "Optimization of filament-wound parts based on non-geodesic winding", Composites Manufacturing, 6, 79-84.

CHAPTER 3: DETERMINATION OF FIBER ORIENTATION ALONG THE LENGTH OF COMPLEX COMPOSITE STRUCTURES SUBJECTED TO INTERNAL PRESSURE AND AXIAL LOADING

A version of this chapter has been accepted as:

Hossain, R., Mertiny, P., Carey, J. P., 2012, "Determination of Fiber Orientation along the Length of Complex Composite Structure Subjected to Internal Pressure and Axial Loading," Proceedings of the ASME 2011 Pressure Vessels & Piping Division Conference, PVP2012, Paper no-PVP2012-78237, July 15-19, 2012, Toronto, Ontario, Canada (Accepted).

CHAPTER 3

3.1 INTRODUCTION

Composite materials provide multiple functionalities that have successfully been employed in the aerospace, marine, automotive, infrastructure and energy industry [1]. Complex-shaped composite structures, such as molded and cast components, possess a wide range of applicability [2]. The manufacturing of these composite components can also be achieved with efficient and robust techniques such as braiding and filament winding by using innovative mandrel systems. These fully automated manufacturing techniques are well suited to produce high performance complex composite structures [3].

Braiding has been used for many applications requiring shaped parts because of structural integrity, design flexibility, damage tolerance, repair ability and low manufacturing cost [4]. Because of its diverse applications and new opportunities in near net shape production, braiding is seeing resurgence in the field of composite manufacturing [5]. On the other hand, filament winding has extensively been used for the manufacturing of axisymmetric cylindrical structures [6].

Designing complex-shaped mandrel geometry to achieve the best combination of part shape and manufacturability is a non-trivial task. It is proposed to develop appropriate design methodologies for complex-shaped mandrels to be implemented in braiding and filament winding production.

Several investigations have been carried out [4-18] to develop models to determine the fiber orientation required for braided and filament-wound composite structures. Brookstein [7] provided a detailed analysis for braided structures where braid reinforcement replaced conventional materials in components such as pressure vessels, rods, shafts, plates and structural columns. The author also provided the optimum fiber orientation for some of these braided structures to satisfy different load carrying requirements. Michaeli and Rosenbaum [8] described a computer control system for a braiding machine, which ensured the desired fiber orientation on a symmetric mandrel; the control algorithm could not adapt the braid angle to changing mandrel diameter. Kessels and Akkerman [9] presented a fast and efficient model to predict fiber angles for complex bi-axially braided preforms; however numerical predictions of the change in braid angle along the mandrel length in regions of changing mandrel cross-section were not accurate.

To effectively use filament winding production capabilities, Mazumdar and Hoa [10-12] presented geometry-based approaches to generate the desired fiber distribution on cylindrical, axisymmetric as well as complex-shaped mandrels. Winding on non-cylindrical mandrel with curved cross-sections was not addressed in their work. Carvalho et al. [6] developed a methodology with integrated numerical analysis for the design of filament-wound parts which included the determination of ideal fiber orientations using finite element analysis; generation of feasible paths; determination of the final lay-up sequence; and an analysis to adapt the final lay-up to meet strength and stiffness requirements. The conical filament wound part was loaded in simple torsion. The methodology required multiple iterations to provide proper solutions; for more complex shaped part, it was suggested that more iterations would be needed.

Composite structures are widely used in applications in which combinations of internal/external pressure, bending, torsion and axial loading may be present. There are various methods for analyzing stresses and strains associated with these loading conditions, including netting [13], finite element [6,14], and orthotropic [15] analysis. Netting analysis is a simple yet expedient approach to design cylindrical filament-wound structures. Orthotropic analysis is used to predict the behavior of a loaded composite structure and determine required fiber orientations [15]. Finite element analysis is performed to define optimal ply stacking, where the final laminate is modeled as layered lamina [14]. The lay-up is then adapted until strength and stiffness requirements are achieved to determine optimum fiber orientation.

An analytical procedure was developed by Wild and Vickers [16] to assess stresses and deformations of three different filament wound structures, i.e. a pressure vessel, a centrifuge rotor, and a flywheel, each under particular loading conditions, to assess the effects of wind angle variation through the cylindrical wall. As an example, using netting analysis for a thin walled cylindrical pressure vessel case, the optimum value of the wind angle was derived as the well-known 54.74°. The authors also reported that the wind angles in each layer can be varied so as to provide both a more even distribution of the strength ratio (i.e. ratio of applied stress to strength) and higher failure pressure. Jones et al. [17] conducted a geometric analysis of the dome of filament wound pressure vessels. They described that the curvilinear fiber path leads to a continuous change in winding angle and laminate thickness. Because the feasibility of a fiber path depends on the surface on which it is wound, winding angles may vary in the longitudinal and thickness direction of a wound structure. Its mechanical behavior was predicted from the fiber alignment and thickness distribution along the dome ended zone of pressure vessel using delta- axisymmetric method, which calculated the winding pattern over the dome. Clearly, an accurate wind angle distribution must be known to precisely predict the behavior of the wound part. Park et al. [18] studied the behavior of cylindrical filament wound pressure vessels subjected to internal pressure as well as the wind angle variation in the dome section. They calculated the fiber angle distribution in the dome section using finite element analysis and quantified the fiber angle change through the thickness direction.

The above literature review presents different methodologies available for predicting the ideal fiber orientations required to satisfying strength and stiffness requirements for conventional braided and filament-wound shapes (e.g. cylindrical piping and pressure vessels) under specific loading conditions. No models were found to provide fiber orientations along the mandrel for the design of complex-shaped structures with variable cross-sections. The aim of the present study is to provide an expedient technique for computing the fiber angle variation along the length of a composite structure having variable cross-section geometry for combined loading conditions. Here a method based on netting analysis theory is presented as an initial approach to determine the fiber orientation along the length of an axially symmetric mandrel for different ratios of axial loading and internal pressure. This work is seen as the foundation for a design framework yielding braiding or filament winding manufacturing parameters for complex-shaped structures subjected to a range of applied loadings.

To meet these objectives, it is necessary to obtain an analytical description of the mandrel surface and determine fiber orientations that satisfy design requirements such as strength and stiffness. These steps are described in the following sections.

3.2 DEFINING MANDREL SURFACE EQUATIONS

Composite structures may be designed to have an intricate geometry that is contoured to a complex mandrel shape. Mandrel shape plays an important role in determining the fiber orientation distribution as they will greatly affect local stresses. Generally, the fiber orientation along the mandrel axis cannot be obtained directly for complex-shaped mandrels. Modeling of relevant mandrel shapes and providing characteristic mandrel surface equations is necessary to determine fiber orientation variation along the mandrel length.

In chapter 2 and in Hossain et al. [19], mathematical expressions were presented for some complex mandrel geometries with cross-section shapes and dimensions that vary along mandrel length representing practical composite structures. These equations will be used here to determine the variation of fiber angle along the length of a composite structure subjected to simple and combined loading conditions.

A brief review on the definition of mandrel surface equations is presented below for two particular cases, as the details derivations were provided in the previous chapter. Geometry and coordinate system (Cartesian shown) for the various mandrel models are defined in Figure 3.1.

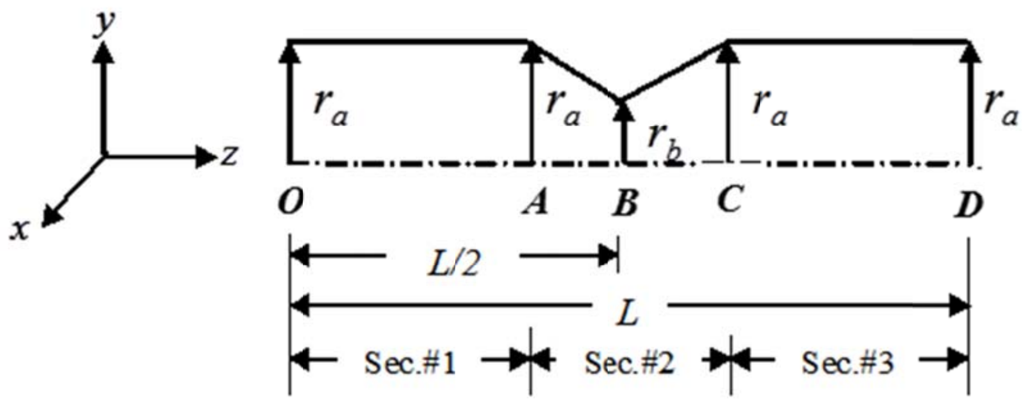

Figure 3.1: General mandrel shape.

In the present study two different complex shape mandrels are considered to find the fiber angle variation along mandrel length. These are shown as solid models in Figure 3.2, for mandrels with circular cross-section with either (a) abruptly or (b) smoothly changing slopes along the converging-diverging mandrel midsection. The surface equations of other mandrels, such as, ellipsoid and rectangular can be implemented as well in order to generate the desired fiber orientation, when subjected to loading conditions.

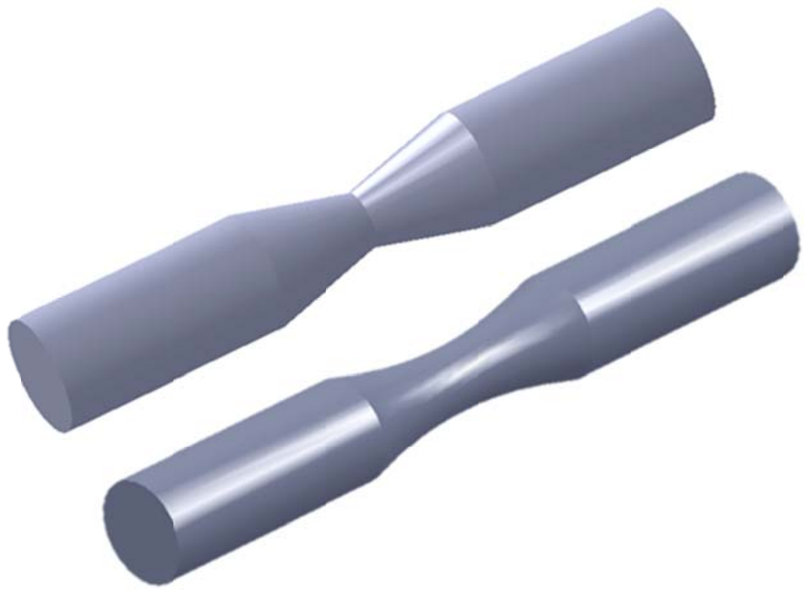

Figure 3.2: Circular mandrel shapes with (a) abruptly (top most) and (b) smoothly (lower most) changing midsection slope.

For the mandrel geometries considered herein, surface equations were developed for each segment. Combining each segment provides a global equation set [19]. For the circular mandrel shape with abruptly changing midsection slope the characteristic equation of the mandrel surface is:

$$r(z) = r_a \times H(t) + \left[K \times r_a + (1-K)r_b\right] \times H(-t) \tag{1}$$

The equation for the circular mandrel cross-section shape with smoothly changing midsection slope is given by:

$$r(z) = r_a \times H(t) + \left[r_a + \sqrt{R^2 - (z_b - z_a)^2} - \sqrt{R^2 - (z_b - z)^2}\right] \times H(-t) \tag{2}$$

where R is the radius of the midsection surface path. R is determined by:

$$R = (1/2)\left[(r_a - r_b) - \frac{(z_b - z_a)^2}{(r_b - r_a)} \right] \tag{3}$$

All other variables are defined in Figure 3.1.

3.3 FIBER ANGLE DETERMINATION USING NETTING ANALYSIS

During the design process, material parameters are selected to ensure that the structure satisfies strength and stiffness requirements. Due to the highly directional nature of continuous fiber reinforcement, it is a common approach to place the fibers in the maximum stress directions. The stress direction is obtained by an appropriate strength of materials analysis along the filament-wound part and throughout the different layers [6]. It shall be emphasized here that the properties of fiber reinforced polymer composites are highly tailorable, allowing a designer to achieve characteristics such as optimal strength at minimum weight. For example, a common notion is that material is effectively wasted for the axial direction of a pressure vessel when fabricating it from an isotropic material since the hoop stress is twice the axial stress within its cylindrical section (considering a thin-walled vessel under closed-end pressure loading) [20]. Constructing a vessel with fiber composites alleviates this problem by placing fibers with a bias in the hoop direction to withstand the higher stress. For the filament winding process, such an optimization implies the appropriate selection of winding angles along the structure, followed by verifying that they can be achieved during the manufacturing process [21].

From among the different possible design methods, netting analysis theory was deemed adequate to determine a suitable fiber orientation and its variation along the length of a complex-shaped mandrel subjected to internal pressure, p, and axial traction loading, F. As such, the following assumptions were made:

- All loads are supported by the fibers in tension only, shear stresses in the composite plies are negligible and any contribution from the matrix material was neglected.
- Fiber architectures considered herein are helical windings oriented at corresponding angles of $\pm\alpha$, representative of braiding and filament winding angle-ply reinforcement strategy.
- Hoop and longitudinal stresses arising from combined loadings were resolved into a single resultant force in the fiber direction.

Considering a circular cross-section structure with variable radius along its length, the mandrel surface equations for $r(z)$, Eqs. (1) and (2), were used in subsequent analyses. The hoop and axial directions are denoted by h and a respectively. The model is based on the physical interpretation that hoop and axial strains can be measured to find the strain, and subsequently, stress along the fiber direction. The fiber strain ε_α at an angle α from the axial direction is given in terms of the hoop and axial strains, ε_h and ε_a, by the following transformation equation:

$$\varepsilon_\alpha = \varepsilon_h \sin^2\alpha + \varepsilon_a \cos^2\alpha + \gamma_{ah} \sin\alpha \cos\alpha \tag{4}$$

The term involving the shear strain, γ_{ha} is neglected for netting analysis since fibers are assumed to be loaded in tension and shear stresses in the composite plies are negligible. The fiber stress can thus be calculated as:

$$\sigma_\alpha = E\varepsilon_\alpha = E(\varepsilon_h \sin^2\alpha + \varepsilon_a \cos^2\alpha) \tag{5}$$

where E is the fiber Young's modulus since any matrix contribution is neglected.

The cross sectional area per unit length of a strand along the layup direction shall be denoted as A_α (i.e. A_α has a dimension of length) [22]. The strand area along the hoop and axial directions per unit length are therefore $A_h = A_\alpha \sin\alpha$ and $A_a = A_\alpha \cos\alpha$, respectively. Using these expressions and the fiber stress given by Eq. (5) the force components per unit length in the hoop and axial directions can respectively be resolved as:

$$F_h = \sigma_\alpha A_\alpha \sin^2\alpha \tag{6}$$

and

$$F_a = \sigma_\alpha A_\alpha \cos^2\alpha \tag{7}$$

Using Eqs. (6) and (7), equations of equilibrium can be established for the internal forces caused by internal pressure and axial traction. The latter is considered in the form of a superposition of forces in axial direction only. Hence force balance considering the mandrel cross-section should be established along both hoop and axial direction as in Figure 3.3. Details derivation can be found in Appendix A.1.

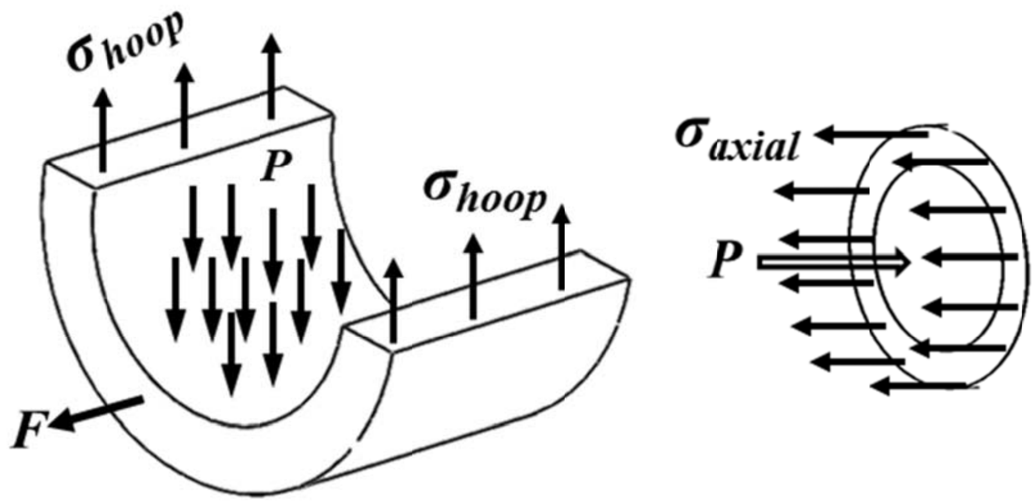

Figure 3.3: (a) Hoop stress and (b) Axial stress developed in the mandrel cross-section due to internal pressure and axial loading.

For the hoop direction the equilibrium equation is:

$$p \times r(z) = \sigma_a \; A_a \sin^2 \alpha \tag{8}$$

$$= \sigma_{hoop} * A$$

Here the area is considered as, $A = L \times t$, and for unit length, L=1, A=t (thickness). Therefore A_α should be assumed as area per unit length [22].

For the axial direction, considering internal pressure and axial traction loading, the equilibrium equation becomes:

$$p\pi(r(z))^2 + F = 2\pi \, r(z)\sigma_a \; A_a \cos^2 \alpha$$

or $$\frac{pr(z)}{2}+\frac{F}{2\pi\, r(z)}=\sigma_a\, A_a \cos^2\alpha \tag{9}$$

$$=\sigma_{axial} * A$$

Dividing Eqs.(8) by (9), an expression for the ratio of hoop to axial stress is derived as:

$$\frac{\sigma_{hoop}}{\sigma_{axial}}=\tan^2\alpha=\frac{pr(z)}{\dfrac{pr(z)}{2}+\dfrac{F}{2\pi\, r(z)}}=\frac{2}{1+\dfrac{1}{\pi\,(r(z))^2}\cdot\left(\dfrac{F}{p}\right)} \tag{10}$$

Therefore, the fiber orientation and its variation along the length of a complex composite structure with variable cross-section radius *r*(*z*), subjected to a combination of internal pressure *p* and axial load *F*, can be determined:

$$\alpha(z)=\arctan\sqrt{\frac{2}{1+\dfrac{1}{\pi\,(r(z))^2}\cdot\left(\dfrac{F}{p}\right)}} \tag{11}$$

3.4 RESULTS AND DISCUSSION

In this section the variation of the fiber angle α (*z*) along the length of the structures shown in Figure 3.2 is considered for different ratios of applied internal pressure and axial loading, *F*/*p*. For clarity these ratios are also expressed in terms of hoop to axial stress, σ_h/σ_a, which is termed by *k*. The intent is to illustrate the effect of cross-sectional geometry and applied loads on the fiber orientation determined through netting analysis.

The stress ratios considered herein are $\sigma_h/\sigma_a = k$ = 2⁄1, 1⁄1, 1/2, 1/4, 1/10. Assuming an internal pressure of unity (i.e. 1 MPa) and a major cross sectional radius of r = 25 mm at point A (i.e. the constant mandrel radius r_a in Figure 3.1), values for the axial load F were determined to obtain the applied loading ratio, F/p, and fiber orientations. Using Eqs. (6) to (9), an expression for F is derived as:

$$F = 2\pi r^2 \left(\frac{1}{k} - \frac{1}{2} \right) \tag{12}$$

Accordingly, F/p ratios for k = 2, 1, 1/2, 1/4, 1/10 are 0 mm^{-2}, 1964 mm^{-2}, 5890 mm^{-2}, 13744 mm^{-2} and 37307 mm^{-2}. Note that units of mm^{-2} for the F/p ratios are omitted herein for convenience. For the various F/p ratios, results for the fiber angle along mandrel length were plotted in Figures 3.4 and 3.5 for the mandrel shapes with abruptly and smoothly changing midsection slope, respectively.

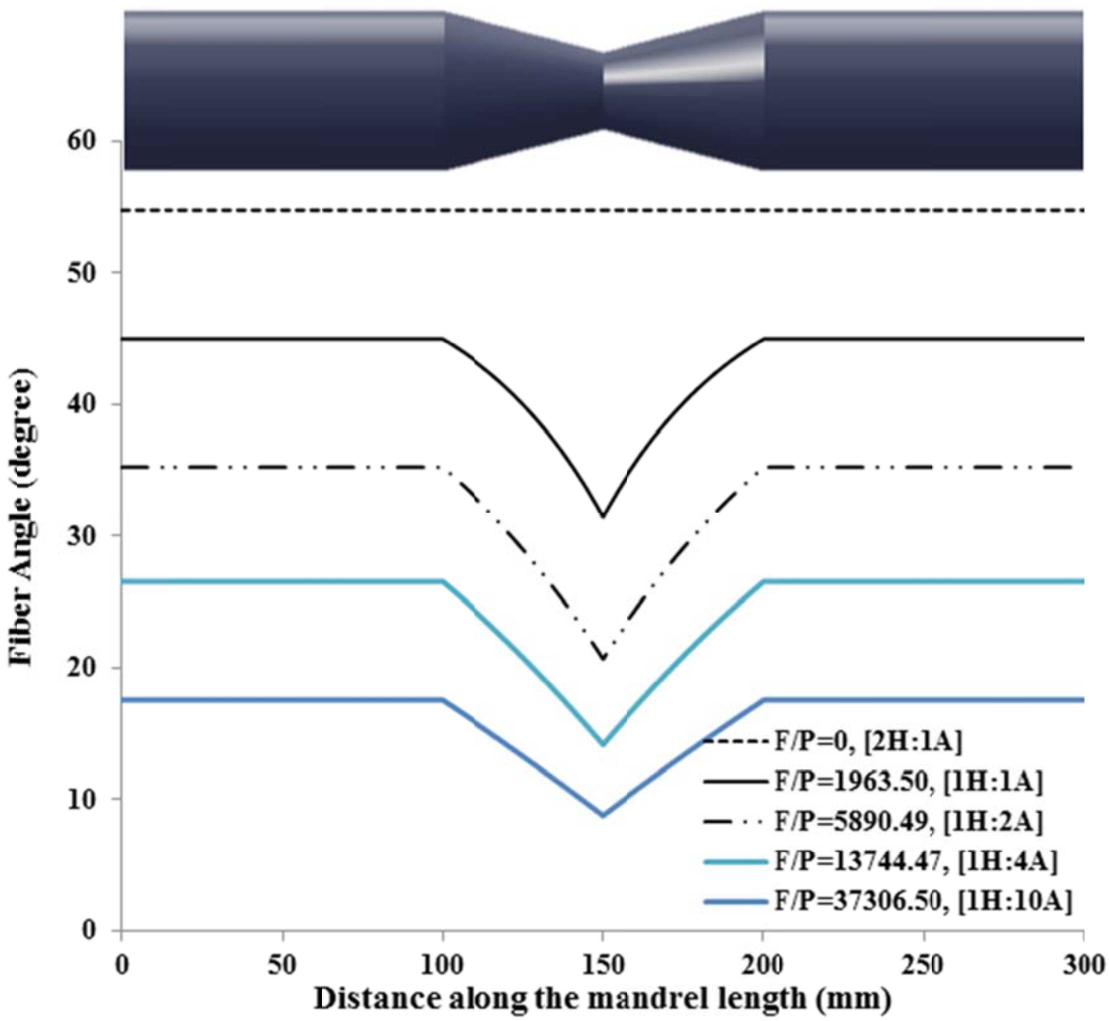

Figure 3.4: Fiber angle variation along the length of a circular cross-section structure with abruptly changing slope in midsection for different ratios of axial load *F* and internal pressure *p*. [square brackets represent the hoop to axial stress ratio].

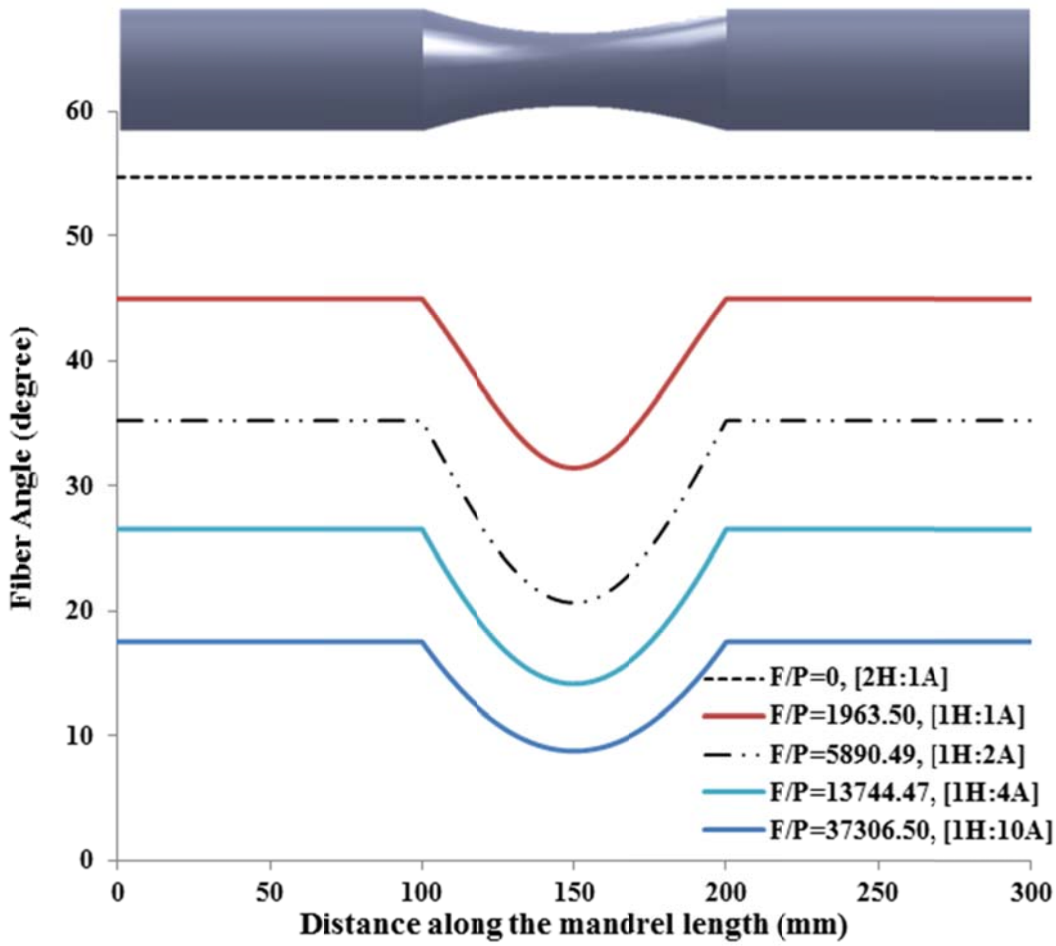

Figure 3.5: Fiber angle variation along the length of a circular cross-section structure with smoothly changing slope in midsection for different ratios of axial load *F* and internal pressure *p*. [square brackets represent the hoop to axial stress ratio].

From Figures 3.4 and 3.5 it can be observed that that the *F*/*p* ratio as well as the change in part geometry may have a significant effect on the fiber orientation along the length of the structure. When $F/p = 0$, i.e. no axial load, Figures 3.4 and 3.5 show that the fiber angle is 54.74°, which is to be expected from netting analysis for a circular structure subjected to only internal pressure. For an increasing axial force, *F*, the fiber angle decreases approaching zero degrees when axial traction loading dominates. This decrease in fiber angle is more pronounced in the converging-diverging midsection. It should be noted here that fiber angles approaching the extremes of 0° and 90° are usually not practical for braiding and filament winding.

Also seen in Figure 3.4 is that along the midsection of the circular cross-section structure with abruptly changing slope some curves are found as linear [1H : 10A] whereas others are curved [1H : 1A]. The reason behind this issue is that according to Eq. (11), α is a function of $r(z)^2$ and F/p. Therefore, when the values of F/p ratios are small, α is dominated by $r(z)^2$ and the variation of α with z along the midsection is parabolic. Conversely, when the values of F/p ratios are greater, α is dominated by F/p, a linear relationship.

3.5 CONCLUSIONS

When designing fiber reinforced composite structures, it is necessary to determine fiber orientation to support applied loads and other design constraints. This is particularly challenging for complex geometries. In this chapter, netting analysis theory was implemented in an initial approach to determine the fiber orientation for structures with circular cross-section and converging-diverging midsections. The approach developed in the chapter provides a relationship between fiber orientation and the internal pressure and axial loading applied to the complex-shaped structure. An extension of this work, presented in the next chapter, will incorporate appropriate material failure criteria to determine the optimal fiber layout for braiding and filament winding manufacturing methods.

3.6 REFERENCES

1. Gibson, F.R., 2010, “A review of recent research on mechanics of multifunctional composite materials and structures”, Composite Structures, 92, 2793–2810.

2. Farin, G., 1990, “Curves and Surfaces for Computer Aided Geometric Design: A Practical Guide”, Academic Press Inc., Boston, MA.

3. Kamiya, R., Cheeseman, B.A., Chou, T.W., 2000, “Some recent advances in the fabrication and design of three-dimensional textile preforms: a review”, Composites Science and Technology, 60, 33-47.

4. Liao, T., Adanur, S., 2000, “3D Structural Simulation of Tubular Braided Fabrics for Net-Shape Composites”, Textile Research Journal, 70, 297-303.

5. Ayranci, C., Carey, J., 2008, “2-D braided composites: a review for stiffness critical applications”, Composite Structures, 85, 43-58.

6. Carvalho, J.D., Lossie, M., Vandepitte, D., Van Brussel, H., 1995, “Optimization of filament-wound parts based on non-geodesic winding”, Composites Manufacturing, 6, 79-84.

7. Brookstein D., 1988, “Structural applications of advanced braided composites”, Proc. SPE/APC’88, Los Angeles, CA, 415–424.

8. Michaeli, W., Rosenbaum, U., 1989, “Structural braiding of complex-shaped FRP parts: A new approach for higher productivity”, 34th International SAMPE Symposium, Covina, CA, 1834-1842.

9. Kessels, J.F.A., Akkerman, R., 2001, “Prediction of the yarn trajectories on complex braided preforms,” Composites A, 33, 1073–1081.

10. Mazumdar, S.K., Hoa, S.V., 1995, “Analytical model for low cost manufacturing of composites components by filament winding, Part1: direct kinematics”, Journal of Composite Materials, 29, 1515-1541.

11. Mazumder, S. K., Hoa, S.V., 1991,”On the kinematics of filament winding on non-axisymmetric cylindrical mandrels, Part 1: A generalized model”, Composites Manufacturing, 2, 23-30.

12. Mazumder, S. K., Hoa, S.V., 1992, “Filament winding on tapered axisymmetric and non-axisymmetric composite components”, 13th International SAMPE Conference, Covina, CA.

13. Engineering Materials Handbook, 1987, ASM International, Metals Park, OH, p. 508.

14. Shiratori, E., Ikegami, K. and Ishii, T., 1981, “Study on the high speed rotating disc reinforced by laminating and hoop winding method”, Bulletin of JSME, 24, 501-506.

15. Lekhnitskii, S.G., 1968, “Anisotropic Plates”, Gordon and Breach Science Publishers, London, United Kingdom.

16. Wild, P.M., Vickers, C.W., 1997, “Analysis of filament-wound cylindrical shells under combined centrifugal, pressure and axial loading”, Composites A, 28, 47-55.

17. Jones, D.T., Jones, I.A., Middleton V., 1996, “Improving composite lay up for non-spherical filament wound pressure vessels”, Composites A, 27, 311-317.

18. Park, J., Hong, C., Kim, C., Kim, C., 2002, “Analysis of filament wound composite structures considering the change of winding angles through the thickness direction”, Composites Structures, 55, 63-71.

19. Hossain, R., Carey, J., Mertiny, P., 2011, “Complex-shaped mandrel modeling for braiding and filament-winding”, 23rd Canadian Congress of Applied Mechanics,, Vancouver, British Columbia, paper no-124.

20. Evans, J.T., Gibson, A.G., 2002, “Composite angle ply laminates and netting analysis”, Proc. Royal Society of London A, 458, 3079-3088.

21. Roylance, D.K., 1976, “Netting analysis for filament wound pressure vessels”, Technical Report 76-3, Composites Division, Army Materials and Mechanics Research Center, Watertown, MA.

22. Kaw, A. K., 1997, “Mechanics of composite materials”, CRC Press, NY.

CHAPTER 4: FAILURE ANALYSIS IN THE DETERMINATION OF CRITICAL FIBER ORIENTATION FOR COMPLEX COMPOSITE STRUCTURE SUBJECTED TO COMBINED LOADING

A version of this chapter will be submitted as:

Hossain, R., Mertiny, P., Carey, J. P., 2012, "Failure analysis in the determination of critical fiber orientation for complex composite structure subjected to combined loading", Journal of Pressure Vessel Technology.

CHAPTER 4

4.1 INTRODUCTION

Structures made from fiber-reinforced polymer composites (FRPC) such as pressure vessels and piping have found growing acceptance and application in industry due to in part their high specific properties and corrosion resistance. Complex-shaped structures provide considerable practicality and effectiveness for many industrial applications, examples of which are molded and cast components [1]. An ever increasing range of applications requires complex-shaped FRPC structures, which in turn necessitates efficient and robust manufacturing methods such as braiding and filament winding. Employing these established manufacturing methods, complex-shaped composite components can be produced in conjunction with innovative mandrel systems.

Composite structures are widely used in applications in which a combination of internal/external pressure, bending, torsion and axial loading may be present. There are various design criteria for analyzing stresses and strains associated with these loading conditions, including netting analysis [2], finite element method [3], and orthotropic analysis [4]. Netting analysis is a simplistic yet expedient approach to the design of cylindrical filament-wound structures. Under the assumption of plane stress, orthotropic analysis may be used to analyze stress and strain and predict the behavior of a composite structure under loading and thus determine fiber orientations [4]. Finite element modeling allows for analyzing a composite laminate as a layered structure. Lamina sequence and fiber orientations can thus be optimized until strength and stiffness requirements are met [3].

Damage in composite structures is a complex phenomenon involving various failure mechanisms. Understanding the failure process and the development of reliable failure criteria is an essential prerequisite for an effective analysis of composite materials [5]. Failure in a composite laminate initiates in the most stressed lamina (with respect to anisotropic material strength), followed by a sequence of next-to-be-most-stressed lamina leading eventually to ultimate failure. To this end, a lamina failure criterion is often used in conjunction with lamination theory to evaluate stress and strains in the various plies. For example, a theoretical and experimental analysis of the strength of $\pm 55^{\circ}$ and $\pm 75^{\circ}$ pipes under biaxial loading of internal pressure and axial force was carried in [5]. In this study, theoretical failure envelopes were obtained using laminate theory and netting analysis. Other extensive research work on failure analysis of laminated composite structures focused on approaches such as non-linear viscoplastic constitutive modeling, fracture mechanics, damage mechanics and macroscopic (global) failure criteria [6].

Linear and quadratic failure criteria have been popular for the design and analysis of composite structures for a variety of industrial applications in which combined loading conditions are present. Srikanth and Rao [7] experimentally determined strength and stiffness properties of both braided and filament wound carbon fiber reinforced polymer composites that were fabricated with varied fiber orientations. They found good correlations between experimental data and predictions made by conventional modeling approaches, such as classical laminate theory (CLT) and the Tsai- Wu failure criterion. Eckold et al. [8] predicted the failure envelopes for filament-wound materials under biaxial loading using a maximum stress failure criterion and found good agreement with experimental results. However, the maximum stress failure criterion was less accurate than the distortional energy failure criterion in assessing material strength under internal pressure and axial loading conditions. Gargiulo et al. [9] delineated the failure behavior of composite tubes under simultaneous internal or external pressure and axial loads producing a variety of biaxial stress conditions. Finite element analysis in conjunction with the Tsai-Wu failure criterion was used to predict specimen failure. Onder et al. [6] investigated the burst pressure of filament-wound composite pressure vessels under alternating pure internal pressure; experimentation was employed to verify optimum winding angles.

The review of the technical literature clearly showed that a failure analysis must be comprehensive for combined and variable loading conditions. Through netting analysis only a single fiber angle can be determined for a specific loading condition, such as a certain ratio between hoop and axial stresses. Such a fiber angle would not necessarily comply with variable loading conditions caused by e.g. internal pressure and axial traction being changed independently from each other. Thus, a design process based on netting analysis (such as presented in Chapter 3 and [10]) should be enhanced with an examination of strength properties for stress conditions that deviate from initial netting analysis results. The technical literature is limited with respect to such a design approach, which provides opportunities for an expedient and efficient design methodology. In the present study an attempt was made to enhance the design methodology of composite structures subjected to combined loads and manufactured by either braiding or filament winding by implementing netting analysis and a suitable quadratic failure criterion to provide a safe and practical design approach that also affords considerable design flexibility. The design process for braided or filament-wound composite structures as described in Chapter 3 and [10] was expanded by implementing a Tsai-Wu failure analysis to ascertain critical fiber orientations and to assess the structure performance and strength. Herein two material systems, i.e. glass fiber/epoxy and carbon fiber/epoxy were considered to explore and compare failure behavior under combined and variable loading conditions.

4.2 TSAI-WU FAILURE ANALYSIS TO DETERMINE CRITICAL WINDING ANGLES

The Tsai-Wu failure criterion was used to determine critical winding angles. In accordance with previous work, i.e. Chapter 3 and [10], a local coordinate system comprised of perpendicular axes ‘1’ and ‘2’ was defined to signify the longitudinal and transverse fiber directions respectively [11]. A global X-Y coordinate system was established where the angle between axes X and ‘1’ is denoted the winding angle α. Therefore, the stress transformation relations between the two coordinate systems can be given as shown in Eq.(1).

$$\begin{Bmatrix}\sigma_1\\ \sigma_2\\ \tau_{12}\end{Bmatrix} = [T]\begin{Bmatrix}\sigma_x\\ \sigma_y\\ \tau_{xy}\end{Bmatrix} = \begin{bmatrix}\cos^2\alpha & \sin^2\alpha & 2\sin\alpha\cos\alpha\\ \sin^2\alpha & \cos^2\alpha & -2\sin\alpha\cos\alpha\\ -\sin\alpha\cos\alpha & \sin\alpha\cos\alpha & \cos^2\alpha-\sin^2\alpha\end{bmatrix}\begin{Bmatrix}\sigma_a\\ \sigma_h\\ 0\end{Bmatrix}$$

$$= \begin{Bmatrix}\sigma_a\cos^2\alpha+\sigma_h\sin^2\alpha\\ \sigma_a\sin^2\alpha+\sigma_h\cos^2\alpha\\ -\sigma_a\sin\alpha\cos\alpha+\sigma_h\sin\alpha\cos\alpha\end{Bmatrix} = \begin{Bmatrix}(\sigma_a-\sigma_h)\cos^2\alpha+\sigma_h\\ (\sigma_a-\sigma_h)\sin^2\alpha+\sigma_h\\ \frac{1}{2}(\sigma_h-\sigma_a)\sin 2\alpha\end{Bmatrix}$$

$$\text{or}\quad \begin{Bmatrix}\sigma_1\\ \sigma_2\\ \tau_{12}\end{Bmatrix} = \begin{Bmatrix}(a-b)\cos^2\alpha+b\\ (a-b)\sin^2\alpha+b\\ \frac{1}{2}(b-a)\sin 2\alpha\end{Bmatrix} \tag{1}$$

where hoop and axial stresses σ_a and σ_h were replaced respectively by the simplified notation of *a* and *b* for convenience.

In the general form of Tsai-Wu failure analysis, a failure index *f* is expressed by

$$f = H_1\sigma_1 + H_2\sigma_2 + H_6\tau_{12} + H_{11}\sigma_1^2 + H_{22}\sigma_2^2 + H_{66}\tau_{12}^2 + 2H_{12}\sigma_1\sigma_2 \tag{2}$$

where components H_1, H_2, H_6, H_{11}, H_{22}, H_{66} and H_{12} are strength parameters of a unidirectional lamina [11]. The failure index *f* is defined such that failure does not occur if $f < 1$. Substituting stresses σ_1, σ_2 and τ_{12} from Eq.(1) into Eq.(2) yields Eq.(3).

$$\begin{aligned} f = {} & H_1\left\{(a-b)\cos^2\alpha+b\right\} + H_2\left\{(a-b)\sin^2\alpha+b\right\} + H_6\left\{\frac{1}{2}(b-a)\sin 2\alpha\right\} \\ & + H_{11}\left\{(a-b)\cos^2\alpha+b\right\}^2 + H_{22}\left\{(a-b)\sin^2\alpha+b\right\}^2 + \\ & H_{66}\left\{\frac{1}{2}(b-a)\sin 2\alpha\right\}^2 + 2H_{12}\left\{(a-b)\cos^2\alpha+b\right\}\left\{(a-b)\sin^2\alpha+b\right\} \end{aligned} \tag{3}$$

Defining a stress ratio k between a and b such that $b = k\,a$, then Eq.(3) becomes,

$$f = a\left[\begin{array}{l} \left\{(k-(k-1)\cos^2\alpha\right\}H_1 + H_2\left\{(k-(k-1))\sin^2\alpha\right\} - H_6\left\{\frac{1}{2}(k-1)\sin 2\alpha\right\} \\ +a H_{11}\left\{(k-(k-1)\cos^2\alpha\right\}^2 + 2a\,H_{12}\left\{(k-(k-1)\cos^2\alpha\right\}\left\{(k-(k-1))\sin^2\alpha\right\} \\ +a\,H_{22}\left\{(k-(k-1))\sin^2\alpha\right\}^2 + H_{66}\left\{\frac{1}{4}a(k-1)^2\sin^2 2\alpha\right\} \end{array}\right] \quad (4)$$

A critical fiber angle $\alpha_{critical}$ is determined by the failure index f so that failure is impending for the different material systems. Table 4.1 shows the strength properties for the two material cases, i.e. E-glass/epoxy (S2-449 43.5k/SP 381) [11] and carbon fibre/epoxy (AS4-12K/938) [12]. In the present analysis it was chosen to vary the values of axial stress a and the ratio between hoop-to-axial stress ratio k. The strength components H_1, H_2, H_6, H_{11}, H_{22}, H_{66} and H_{12} for the Tsai-Wu failure index in Eq. (2) given in Table 4.2 were determined according to [13] using respective strength data for both materials.

It should be noted here that the present approach deliberately ignores any load sharing contribution from adjacent laminae, which would have the same fiber angle but with negative inclination. In other words, it is assumed that each lamina carries identical stresses, i.e. the average hoop and axial stress of the structure. Considering strain continuity in the different laminae of a laminate it becomes apparent that stresses in the directions parallel and transverse to the fibers would not develop in the same manner as when assuming a fully independent lamina. The reason the present analysis approach was chosen is that it ensures conservative designs by ignoring load sharing effects.

Table 4.1: Material strength properties

Material Properties	Glass fiber /epoxy	Carbon fiber /epoxy
Ultimate longitudinal tensile strength $(\sigma_1^T)_{ult}$, (MPa)	1062	1875
Ultimate longitudinal compressive strength $(\sigma_1^C)_{ult}$, (MPa)	610	1455
Ultimate transverse tensile strength $(\sigma_2^T)_{ult}$, (MPa)	31	62
Ultimate transverse compressive strength $(\sigma_2^C)_{ult}$, (MPa)	118	210
Ultimate in plane shear strength $(\tau_{12})_{ult}$, (MPa)	72	90

Table 4.2: Components for determining the Tsai-Wu failure index

Component	Expression	Glass fiber /epoxy	Carbon fiber /epoxy
H_1 (MPa)$^{-1}$	$\frac{1}{(\sigma_1^T)_{ult}} - \frac{1}{(\sigma_1^C)_{ult}}$	-6.977×10^{-4}	-1.542×10^{-4}
H_2 (MPa)$^{-1}$	$\frac{1}{(\sigma_2^T)_{ult}} - \frac{1}{(\sigma_2^C)_{ult}}$	0.0238	0.011
H_6 (MPa)$^{-1}$	$H_6=0$	0	0
H_{11} (MPa)$^{-2}$	$\frac{1}{(\sigma_1^T)_{ult}(\sigma_1^C)_{ult}}$	1.544×10^{-6}	3.665×10^{-7}
H_{22} (MPa)$^{-2}$	$\frac{1}{(\sigma_2^T)_{ult}(\sigma_2^C)_{ult}}$	2.734×10^{-4}	7.723×10^{-5}
H_{66} (MPa)$^{-2}$	$\frac{1}{(\tau_{12})_{ult}^2}$	1.93×10^{-4}	1.245×10^{-4}
H_{12} (MPa)$^{-2}$	$-\frac{1}{(\sigma_1^T)_{ult}^2}$	-4.433×10^{-7}	-1.422×10^{-7}

4.3 RESULTS AND DISCUSSION

In the first part of the examination the variation of the failure index f with fiber angle α is presented for varying axial stress values while maintaining a constant hoop-to-axial stress ratio. The different ratios of applied axial loading and internal pressure F/p are expressed in terms of hoop-to-axial stress ratios k for convenience. The loading case of $F/p = 10$ was assumed herein, and the mandrel cross-section radius was taken as $r = 12$mm (at point B along the z-direction, see Figure 3.1 in Chapter 3). Thus, according to Eq. (10) in Chapter 3, $k = 1.96$. Results for the failure index are shown for glass fiber/epoxy and carbon fiber/epoxy materials in Figures 4.1 and 4.2 respectively. Similar trends for the failure index with varying fiber angle can be observed for axial stress values a ranging correspondingly from 10 MPa to 32 MPa (glass/epoxy) and 10 MPA to 64 MPa (carbon/epoxy). A safe design is given for a failure index of $f < 1$ indicated by the dotted line in the figures (i.e. termed herein the 'safe design line' or 'failure line'). Figure 4.1 shows that for axial stresses up to $a = 16$ MPa any fiber angle from 0° to 90° is possible without failure. For any $a > 16$ MPa failure index curves cross the safe design line. When $a > 32$ MPa the failure index curve remains entirely above the safe design line. The intersection of failure index curve and safe design line determines the critical fiber angle $\alpha_{critical}$, which signifies the smallest fiber angle that ensures no failure. For example, when a = 22 MPa $\alpha_{critical}$ is found as 49.5° for glass fibre/epoxy (see Figure 4.1); for carbon fiber/epoxy, $\alpha_{critical}$ is 42.3° for an axial stress value of 40 MPa (Figure 4.2). Moreover, for the present case of $k = 1.96$ the glass/epoxy and carbon/epoxy materials will fail for all fiber angles when $a > 32$ MPa and $a > 64$ MPa respectively.

Similar to the preceding investigation a second assessment of failure index with respect to fiber angle and critical fiber angle $\alpha_{critical}$ was conducted, the difference being that axial stress was kept constant while varying the stress ratio k. Corresponding data for different k values for a fixed axial stress value of $a = 20$ MPa are shown in Figures 4.3 and 4.4 for glass fiber/epoxy and carbon fiber/epoxy, respectively.

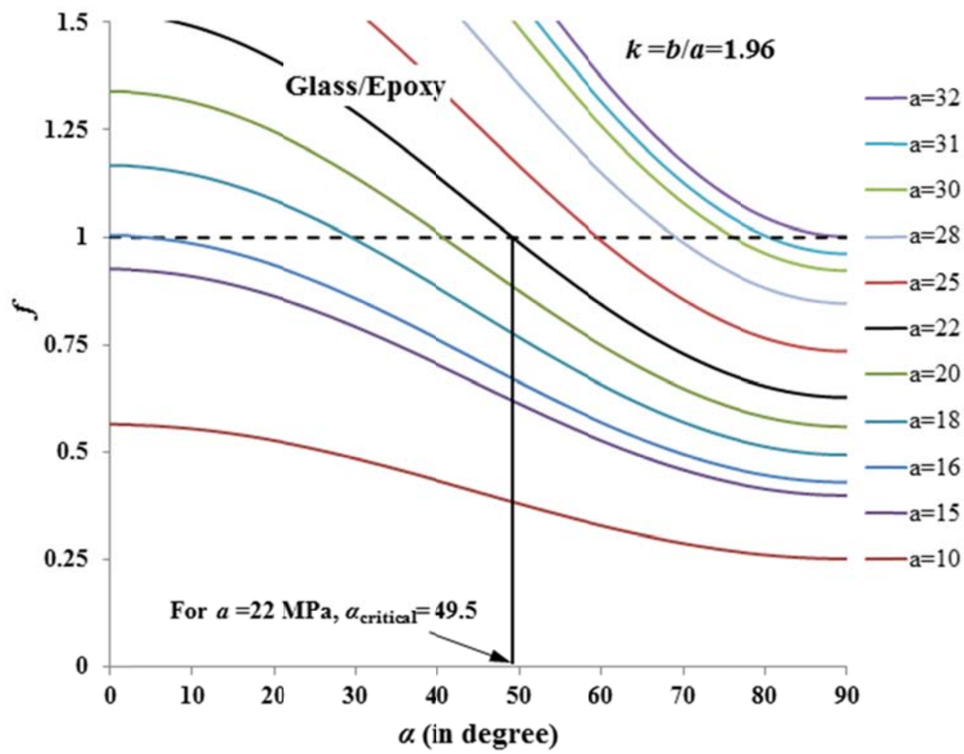

Figure 4.1: Variation of failure index f with fiber angle α in glass/epoxy for a constant stress ratio k and different axial stresses, with failure line at $f = 1$.

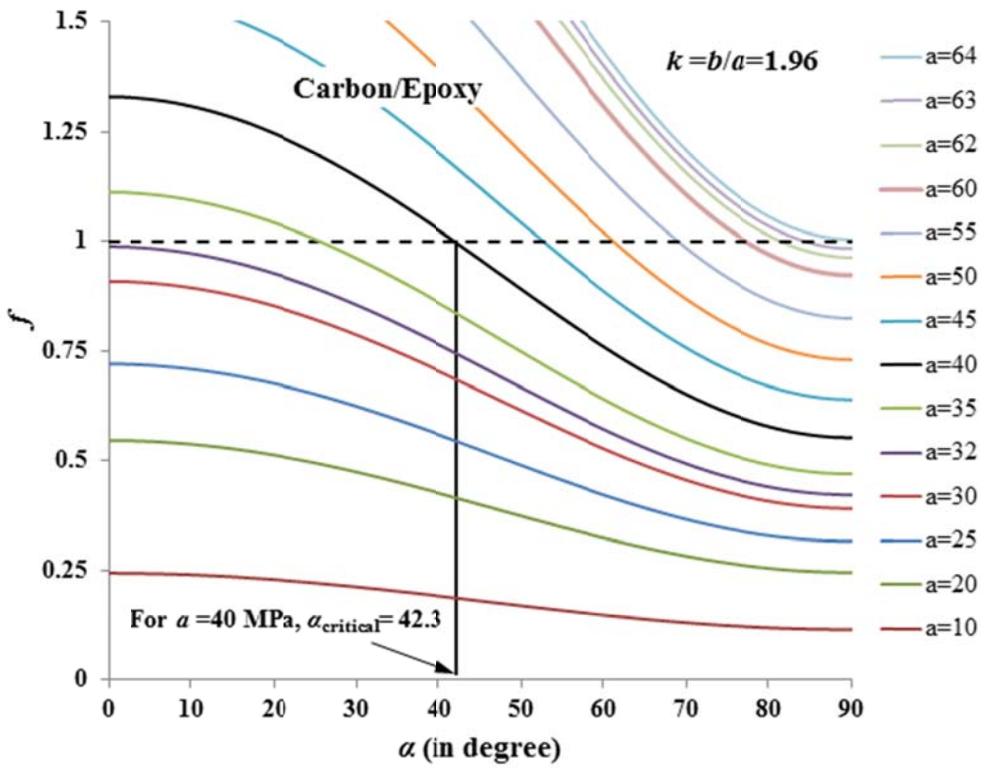

Figure 4.2: Variation of failure index f with fiber angle α in carbon/epoxy for a constant stress ratio k and different axial stresses, with failure line at $f = 1$.

Noteworthy insights for design purposes can be gained from Figures 4.3 and 4.4. The data for glass fiber/epoxy (Figure 4.3) and carbon fiber/epoxy (Figure 4.4) show that all winding angles are feasible for any stress ratios k less than correspondingly 1.57 and 3.16. For higher k a critical fiber angle can be found. Taking for example $k = 4$ the α_{critical} are 66.6° and 37.8° for glass fiber/epoxy (Figure 4.3) and carbon fiber/epoxy (Figure 4.4) respectively. Failure will not occur for angles greater than these critical angles for any given stress ratio k unless $k > 40$ for glass fiber/epoxy and $k > 84$ for carbon fiber/epoxy, which constitute limit hoop-to-axial stress ratios at which the materials will always fail.

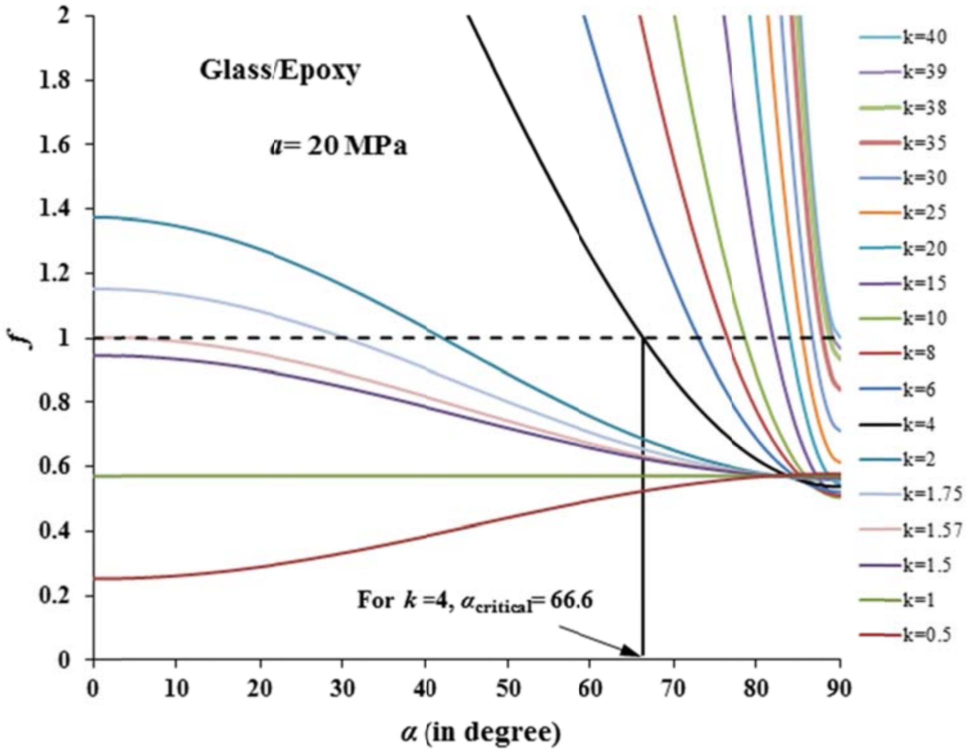

Figure 4.3: Variation of failure index f with fiber angle α in glass/epoxy for a constant axial stress a and different stress ratios k, with failure line at $f = 1$.

Critical fiber critical angles over a range of axial stresses as shown in the separate graphs in Figures 4.1 (glass fiber/epoxy) and 4.2 (carbon fiber/epoxy) were compiled into a single graph in Figure 4.5 (stress ratio of $k = 1.96$) to provide more concise information. Similarly, using data from Figures 4.3 and 4.4, critical fiber angles over a range of stress ratios and a fixed axial stress of $a = 20$ MPa were plotted for both material systems into a single graph, which is presented in Figure 4.6.

From Figure 4.5 it is found that for glass fiber/epoxy and carbon fiber/epoxy the critical angle curves intersect the abscissa (i.e. $\alpha_{critical} = 0º$) at approximately $a = 16$ MPa and $a = 32$ MPa respectively, whereas from Figure 4.6

corresponding values for the hoop-to-axial stress ratio are $k = 1.57$ and $k = 3.16$. Below these a and k values a design will not fail for any given fiber angle. Conversely, for the maximum possible fiber angle of 90º, limiting a and k exist beyond which no fiber angle provides a feasible design. For example, this limiting value is $a = 32$ MPa for glass fiber/epoxy as shown in Figure 4.5, and thus for a between 16 MPa to 32 MPa a safe fiber design is delineated by the critical fiber angle curve. In other words, any design point to the left of the critical fiber angle curves ($f < 1$) can be interpreted as a safe design, while the right side ($f > 1$) indicates failure. In both figures, these regions are greater for carbon fiber/epoxy as would be expected from this stronger and stiffer material.

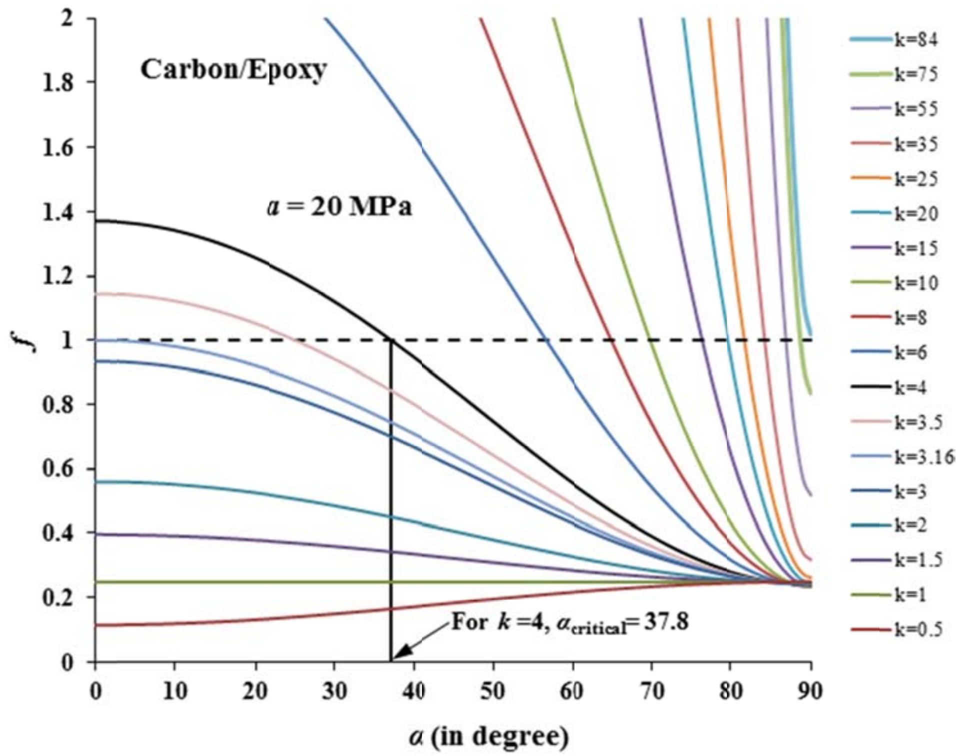

Figure 4.4: Variation of failure index f with fiber angle α in carbon/epoxy for a constant axial stress a and different stress ratios k, with failure line at $f = 1$.

Regarding Figure 4.5 one might expect that with increasing axial stress a the critical fiber angle α_{critical} should tend to 0 degree as this would align the fibers in the axial direction. However, Figure 4.5 shows a different trend for the following reason. It is important to note that k is defined as the ratio of hoop-to-axial stress, meaning that for an increasing axial stress the hoop stress increases proportionally. Consequently, the critical fiber angle is affected by the axial and hoop stresses simultaneously, causing α_{critical} to tend to 90º for an increasing a and $k > 1$.

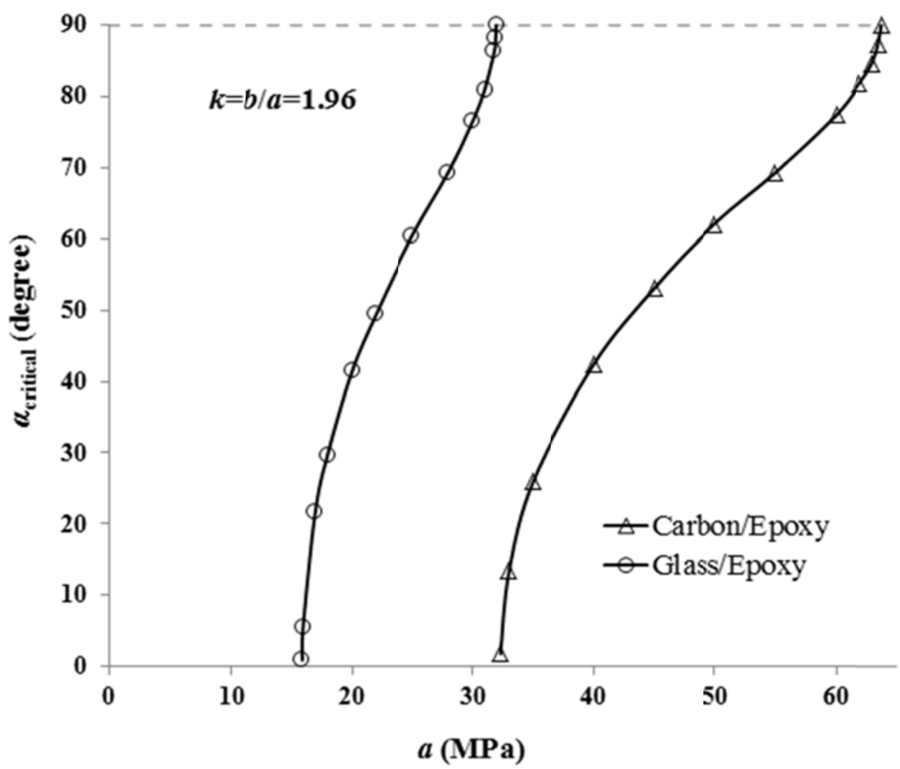

Figure 4.5: Variation of critical fiber angle α_{critical} with axial stress a in glass/epoxy and carbon/epoxy for a constant stress ratios k = 1.96.

Data compiled in Figure 4.6 provides design guidance similar to the graph in Figure 4.5. Hoop-to-axial stress ratios of $k < 1.6$ and $k < 3.2$ constitute limiting values below which all fiber angles provide a safe design for glass fiber/epoxy and carbon fiber/epoxy respectively. With increasing k values (increasing hoop stress; axial stress is a constant 20 MPa for Figure 4.6) the feasible fiber angles increase rapidly towards a pure hoop direction. For example, when $k = 5$ the critical angle is 70° for glass fiber/epoxy. When k reaches values of 39.9 and 83.0 correspondingly for glass fiber/epoxy and carbon fiber/epoxy the critical angle is 90°, which indicates (noting that fiber angles cannot exceed 90°) that for greater k the failure index will exceed unity constituting failure.

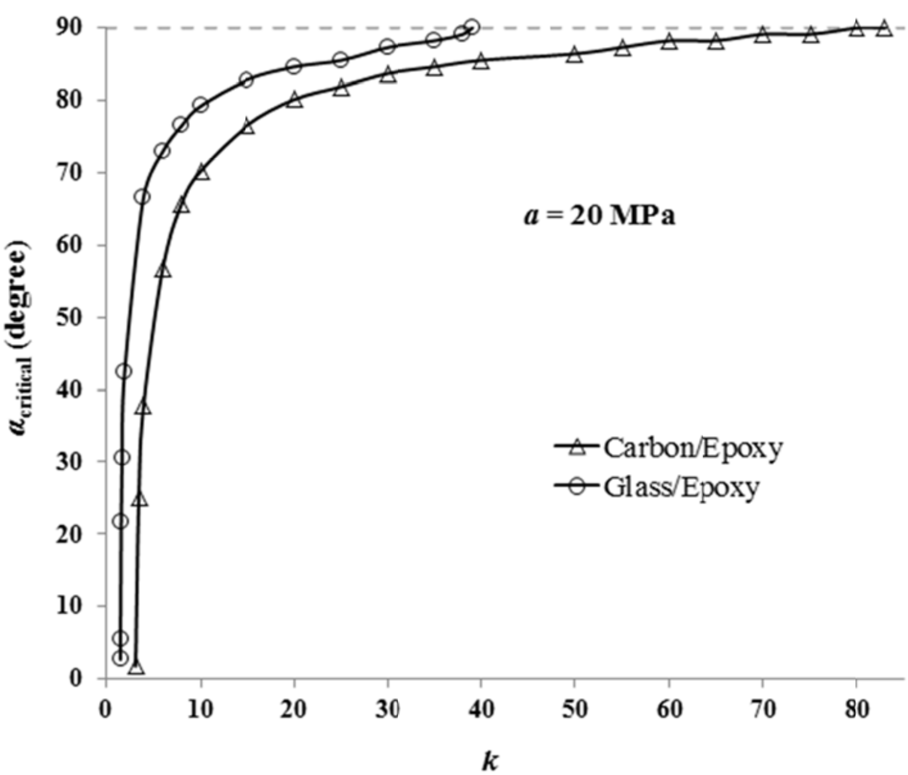

Figure 4.6: Variation of critical fiber angle $\alpha_{critical}$ with hoop-to-axial stress ratio k in glass/epoxy and carbon/epoxy for an axial stress a = 20 MPa.

Critical design data can be condensed further as shown in Figures 4.7 and 4.8. Figure 4.7 depicts $\alpha_{critical}$ over a range of k values for different constant axial stresses, i.e. $a = 10$, 20, 30 MPa. Similarly, Figure 4.8 compiles critical fiber angles for a range of axial stresses for constant stress ratios of $k = 1.96$, 4 and 10.

Figure 4.7 shows that for higher constant axial stress values the $\alpha_{critical}$ versus k curves shift toward the left side of the graph indicating a narrowing safe design zone. For example, the maximum allowable k for glass fiber/epoxy for an axial stress $a = 30$ MPa equals 20 whereas a significant higher k of 80 is possible for $a = 10$ MPa. Note that for the limiting case of zero axial stress (pure hoop stress), i.e. k becomes infinity, no solution can be obtained. In such a case a design curve based Eq.(3) instead of Eq.(4) may be used.

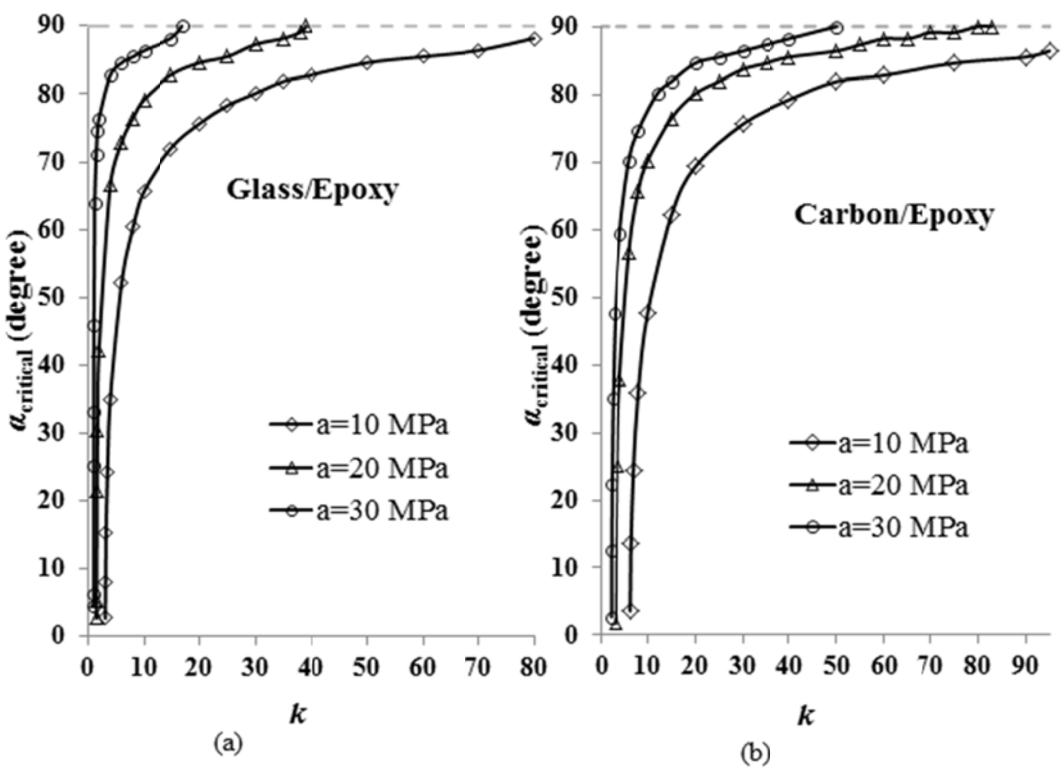

Figure 4.7: Variation of $\alpha_{critical}$ with stress ratio k in (a) glass/epoxy and (b) carbon/epoxy for constant axial stresses of a = 10, 20 and 30 MPa.

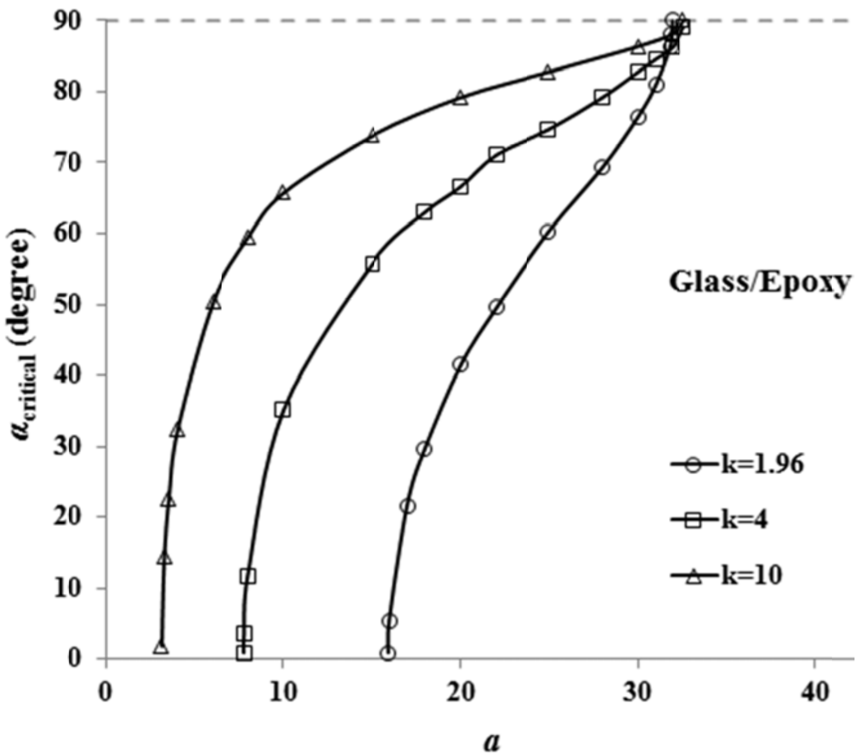

Figure 4.8: Variation of $\alpha_{critical}$ with axial stress *a* in glass/epoxy for constant hoop-to-axial stress ratios *k* = 1.96, 4 and 10.

The span between limiting axial stress values for $\alpha_{critical} = 0^o$ and 90^o degrees should increase for rising *k* (if $k > 0$). This is clearly shown in Figure 4.8, i.e. the span between axial stress values at $\alpha_{critical} = 0^o$ and 90^o (i.e. the end point of each curve) are 16 MPa, 24.8 MPa and 29.5 MPa for stress ratios *k* = 1.96, 4 and 10 respectively. If *k* is increased further, this range will also become larger.

Interesting results can also be obtained for a stress ratio *k* = 0, meaning the absence of hoop stress. In this case $\alpha_{critical}$ will approach 0^o with increasing axial stress *a*, which is clearly shown in Figure 4.9.

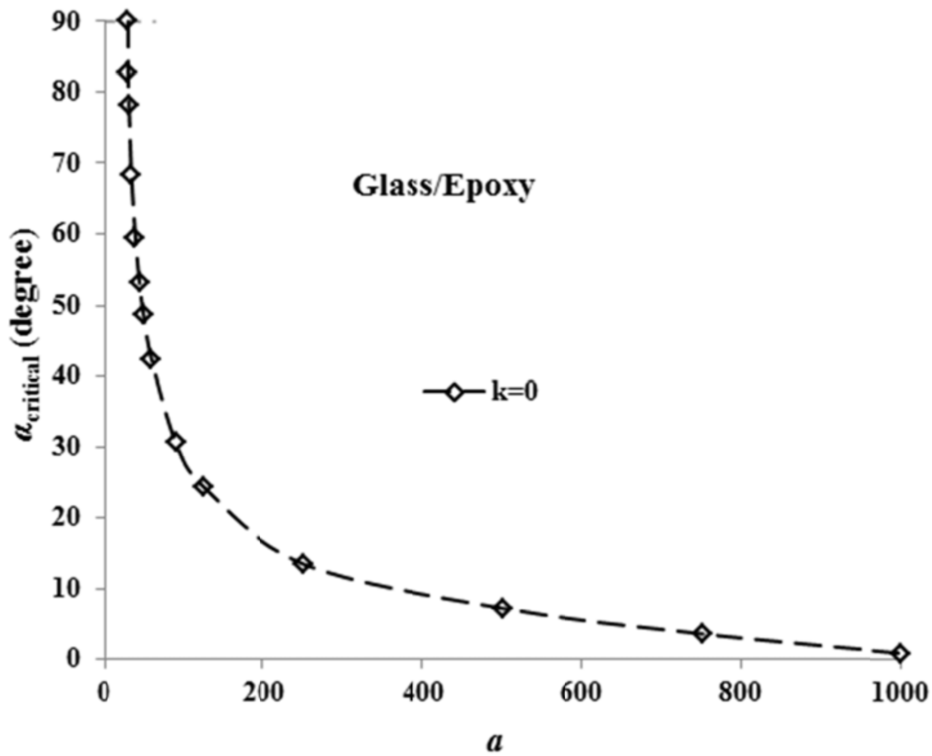

Figure 4.9: Variation of $\alpha_{critical}$ with axial stress a in glass/epoxy for pure axial loading (k = 0).

The analysis presented in Figure 4.9 is similar to work by Srikanth and Rao [7]. As mentioned earlier they determined elastic and strength properties of filament-wound and braided structures experimentally with specimen made with fiber angles ranging from 2° to 88° under tensile loading. In conjunction with their experimental work they presented strength predictions for 0°, 15°, 30°, 45°, 60°, 75° and 90° based on CLT and the Tsai-Wu failure criterion. Predictions were in good agreement with experiments. Critical fiber angles were herein determined for this loading case (k = 0) based on uniaxial strength data given in [7], and results are presented and compared to the work by Srikanth and Rao [7] in Figure 4.10.

It is clearly seen from Figure 4.10 that curves describe a similar trend and converge and coincide towards the extremes of the critical fiber angles (i.e. 0º and 90º). Nevertheless, the curves diverge considerable for angles greater than zero and less than about 45º, that is, the present analysis provides conservative data. Such an outcome was to be expected considering the present analysis neglected any reinforcement effects from adjacent plies (single lamina analysis) whereas Srikanth and Rao [7] based their predictions on two-ply filament-wound structures using CLT. Nevertheless, in the present context it is considered favorable using conservative data to provide design guidance.

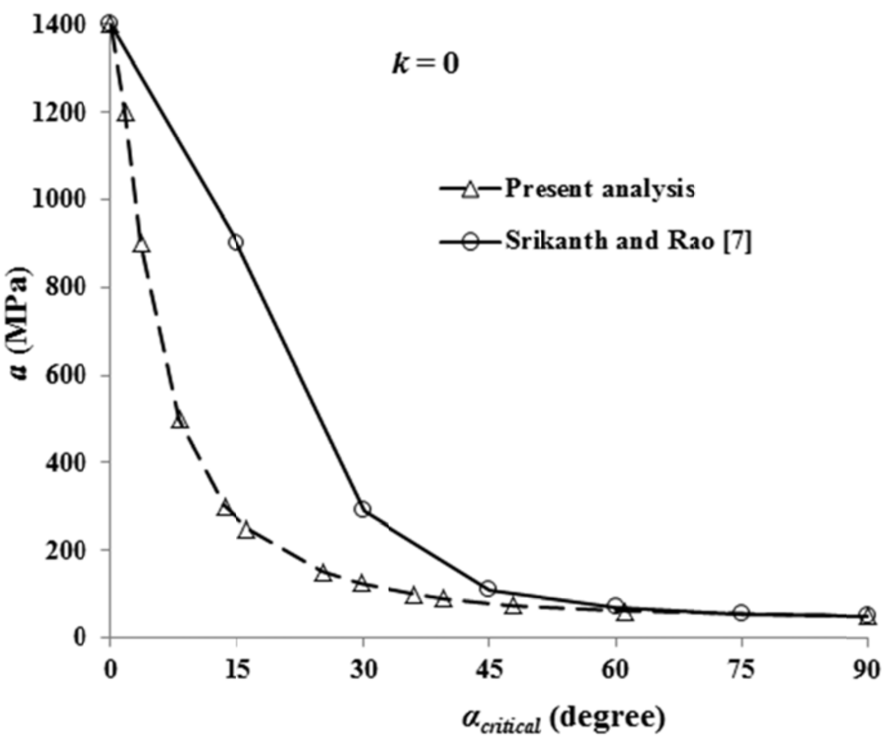

Figure 4.10: Comparison of α_{critical} from present analysis with results by Srikanth and Rao [7] for pure axial loading (k = 0).

Preceding analyses clearly demonstrate that a composite structure featuring a single specific cross-ply fiber architecture may able sustain variable loading conditions, provided that strength limits are not violated. Netting analysis as applied in Chapter 3 is a convenient approach to determine fiber angles for complex-shaped filament-wound or braided structures. The caveat associated with this method is its inability of capturing variable loading conditions, which quite possibly may occur during the operation of such structures. An approach based on a comprehensive failure theory as described in this section enables an expedient and convenient design process in which netting analysis can be applied for the initial design of complex structures. Multiaxial failure analysis and the notion of critical fiber angles can then be employed in a subsequent step or in an iterative fashion to validate the suitability of the initial fiber architecture found by netting analysis. For this to occur a designer requires knowledge of material strength properties and the target and additionally possible loading conditions for the analysis input. In this fashion an expedient and convenient design methodology can be established.

4.4 CONCLUSIONS

The design of filament-wound or braided composite structures includes the determination of the fiber orientation based on applied loads and other design constraints. This is particularly challenging for complex geometries. In this chapter, Tsai-Wu failure theory was employed to assess critical fiber angles at which applied loadings would cause a structure to fail. The developed methodology is conservative in nature, and it supplements the design process based on netting analysis described in Chapter 3. In combination, netting analysis and the failure theory based approach constitute a design process for complex-shaped structures that is expedient and convenient in nature since mathematical processes are relatively simple; underlying theory is well established and material properties can be obtained with relative ease experimentally or from the technical literature.

4.5 REFERENCES

1. Farin, G., 1990 "Curves and Surfaces for Computer Aided Geometric Design: A Practical Guide", Academic Press Inc., Boston, MA.

2. Engineering Materials Handbook, 1987, ASM International, Metals Park, OH, p. 508.

3. Carvalho, J.D., Lossie, M., Vandepitte, D., Van Brussel, H., 1995, "Optimization of filament-wound parts based on non-geodesic winding", Composites Manufacturing, 6, 79-84.

4. Lekhnitskii, S.G., 1968, "Anisotropic Plates", Gordon and Breach Science Publishers, London, United Kingdom.

5. Soden, P.D., Kitching, R., Tse, P.C., 1989, "Experimental failure stresses for $\pm 55^{\circ}$ filament wound glass fiber reinforced plastic tubes under biaxial loads," Composites, 20(2), 125-135.

6. Onder, A., Sayman, O., Dogan, T., Tarakcioglu, N., 2009, "Burst failure load of composite pressure vessels", Composites Structures, 89(1), 159-166.

7. Srikanth, L., Rao, R.M.V.G.K., 2011. "Concurrent studies on braided and filament wound carbon fiber composites - a comparative appraisal", Journal of Reinforced Plastics & Composites, 30(16), 1359-1365.

8. Eckold, G.C., Leadbetter, D., Soden, P.D., Griggs, P.R., 1978, “Lamination theory in the prediction of failure envelopes for filament wound materials subjected to biaxial loading,” Composites, 9(4), 243-246.

9. Gargiulo, C., Marchetti, M., Rizzo, A., 1996, “Prediction of failure envelopes of composite tubes subjected to biaxial loadings,” Acta Astronautica, 39(5), 355-368.

10. Hossain, R., Mertiny, P., Carey, J.P., 2012, “Determination of fiber orientation along the length of complex composite structures subjected to internal pressure and axial loading,” Proceedings of the ASME 2012 Pressure Vessels & Piping Division Conference PVP2012, July 15-19, 2012, Toronto, Ontario, Canada, Paper No. PVP2012-78237.

11. Kaw, A.K., 1997, Mechanics of Composite Materials, CRC Press, NY.

12. Military Handbook, 2002, MIL-HDBK-17-2F: Composite Materials Handbook, Volume 2 - Polymer Matrix Composites Materials Properties.

13. Tsai, S.W., Wu, E.M., 1971, “A general theory of strength for anisotropic materials”, Journal of Composite Materials, 5(1), 58-80.

14. Tsai, S.W., Hahn, H.T. 1980, Introduction to Composite Materials, Technomic Publishers, Lancaster, PA.

CHAPTER 5
DISCUSSIONS AND CONCLUSIONS

The overarching objective of the proposed research was to develop an expedient and efficient design method for the design of braided and filament wound axisymmetric composite structures with variable cross-section geometry along their length. Specifically, the motivations and objectives were to propose a methodology for the braiding and filament winding techniques that simultaneously focuses on the analytical description and design of complex shape mandrel surfaces; the analysis of fiber orientations for preliminary design requirements; and a thorough investigation of failure analysis methods to assess the structure performance and strength under combined loading conditions (i.e. axial loading and internal pressurization), and provide critical fiber angles at which failure is impending. Employing multi-axial failure analysis and the notion of critical fiber angles it was intended to validate the suitability of the initial fiber architecture found by netting analysis.

5.1 SUMMARY

The major findings of the present research can be summarized as follows:

- Axially symmetric complex shaped mandrels with varying dimensions and cross-sections along their length were designed. Using Solid Works computer aided design software, solid models of four complex shape mandrels were developed that meeting some complex shape requirements, i.e. mandrels with circular cross-section and diameter following an abruptly and smoothly changing slope along the midsection, ellipsoid mandrels and rectangular mandrels. Characteristic mandrel surface equations were developed to define these complex mandrel shapes.

- An expression was derived to provide the relationship between fiber orientation and loading conditions applied to complex shape mandrels with variable cross-section along the midsection by implementing netting analysis theory. Netting analysis is rarely associated with braiding; therefore this methodology was considered primarily for filament winding. Upon further investigation and validation it is conceivable that the work presented herein also provides an approach suitable for braiding; however, such development was beyond the scope of this thesis. Also it should be noted that only mandrels with circular cross-section and diameter following an abruptly and smoothly changing slope along the midsection were considered in this analysis. The variation of the fiber angle for different hoop-to-axial stress ratios was only evaluated for these two mandrel shapes. Developed expressions are functions of axial load to pressure ratio (F/p) and mandrel surface radius, $r(z)$. Therefore, implementing other mandrel geometries should provide some similar results but may require special attention to specific mandrel features (such as sharp changes geometry).

- It was found that the *F*/*p* ratio and changes in mandrel geometry have a significant effect on the fiber orientation along the length of the structure. For clarity *F*/*p* ratios were also expressed in terms of hoop-to-axial stress, σ_h/σ_a. When $F/P = 0$, meaning pure internal pressure and no axial load is applied, the fiber angle becomes 54.74°, which is the expected result from netting analysis for a circular structure subjected to internal pressure only . For an increasing axial force, *F*, the fiber angle decreases, and this decrease is more pronounced in the converging-diverging midsection.
- An attempt was made to enhance the design methodology for composite structures subjected to combined loads by implementing a suitable quadratic Tsai-Wu failure criterion to ascertain critical fiber orientations and to assess the structure performance and strength. The developed methodology involved the determination of a failure index *f* as well as a critical fiber angle α to avoid failure for different materials. Glass fiber/epoxy and carbon fiber/epoxy were used as case studies. Again, the analysis focuses mainly on filament winding, as the braiding process may require a methodology for determining the critical angle that possibly needs to consider strong fiber interlacing. The methodology developed herein can thus only been seen as an approximate approach for braiding unless further validation has been conducted.

  Aforementioned case studies showed that for a given axial load all fiber angles are feasible below a limiting stress ratio *k*. Critical fiber angles were computed for a range of axial stresses. Failure will not occur for angles greater than these critical angles for any given stress ratio *k.* Similarly, critical angle curves can be derived for a given stress ratio. The abscissa intersects of these curves (i.e. $\alpha_{\text{critical}} = 0^{\circ}$) indicate that a design will not fail for any given fiber angle below these axial stress values.

- Critical fiber angle curves can be interpreted such that any design point to the left of a curve ($f < 1$) constitutes a safe design, while the right side ($f > 1$) indicates failure. The safe design zone was found to be greater for carbon fiber/epoxy as would be expected from this stronger and stiffer material.
- Since the presented analyses are based on hoop-to-axial stress ratios for biaxial loadings the hoop stress necessarily increases proportionally with the increase of axial stress. Thus the critical fiber angle is affected by the axial and hoop stresses simultaneously, causing α_{critical} to tend to 90º for an increasing a and $k > 1$.
- For rising axial stress values the α_{critical} versus k curves shift toward the left side of the critical fiber angle graph indicating a narrowing safe design zone.
- For the limiting case of zero axial stress (pure hoop stress), i.e. k becomes infinity and no solution is obtained in this case. Also, interesting results can be found for a stress ratio $k = 0$, meaning the absence of hoop stress. In this case α_{critical} will approach 0º with increasing axial stress.
- The present analysis provides conservative data as it neglects any reinforcement effects from adjacent plies (single lamina analysis). However

it is considered favorable using conservative data to provide design guidance.

5.2 CONTRIBUTIONS

The proposed research contributes to the field of study in several ways:

- The development of characteristic mandrel surface equations for four different complex-shaped mandrels for braiding and filament winding using an analytical technique is a significant step towards generating fiber orientations along the length of the mandrel.

- An expedient theoretical study was conducted for determining the fiber angle variation along the length of a mandrel with variable cross-section considering different ratios between axial load and internal pressure. This work represents the foundation for a design framework providing the manufacturing parameters for complex-shaped filament-wound structures subjected to a range of applied loadings using netting analysis.
- A single fiber angle can be determined through netting analysis for a specific loading condition, such as a certain ratio between hoop and axial stresses. Such angle would not necessarily comply with variable loading conditions caused by internal pressure and/or axial loading being changed independently from each other. To fulfill design requirements for filament-wound structures a Tsai-Wu failure criterion was incorporated to

assess feasible fiber angles under variable loadings. Thus an expedient and convenient design methodology can be established, which demonstrates that a composite structure featuring a simple cross-ply fiber architecture may be able to sustain variable loading conditions, provided that strength limits are not violated.

5.3 FURTHER RECOMMENDATIONS

The findings of this research make a valuable contribution to the design of braided and filament wound complex composite structures. Further investigations in this context are however recommended to overcome limitations of present analyses.

- Analyses for the design of complex-shaped structures were carried out mainly for two particular mandrel geometries, i.e. mandrels with circular cross-section and diameter following an abruptly and smoothly changing slope along the midsection. Similar work should be performed for other complex mandrel shapes with variable cross-sections, such as ellipsoid and rectangular mandrels.
- In this thesis it was chosen to compute results related to biaxial loading for combinations of applied axial stresses and hoop-to-axial stress ratios. Corresponding analyses could also be performed for applied hoop stresses in conjunction with hoop-to-axial stress ratios, which may be useful for certain design problems (e.g. when internal pressurization is a dominating design parameter).

- The developed methodology may be applied to any other composite material system for a variety of loading conditions apart from glass fiber/epoxy and carbon fiber/epoxy. The approach can also be employed with other failure criteria, e.g. maximum stress and maximum strain failure theory.
- It should be noted that instead of netting analysis Tsai-Wu failure theory and similar methods may be implemented to find the variation of fiber angle along the length of a mandrel.
- Much of the work presented herein focused on filament winding because of its simpler fiber architecture. The work should be expanded to braiding which generally features considerable fiber interlacing
- Two-dimensional braiding and filament winding are processes seldom used for manufacturing complex-shaped fiber-reinforced polymer composites because of the difficulty of mapping strand paths to obtain desired full or partial coverage during production. To make these processes more competitive, an expedient method for deriving the fiber path trajectory in order to analytically map the surface of different complex-shaped mandrel geometries subjected to certain loading conditions would be very beneficial.
- Finally, it is recommended to develop an analytical model that relates machine process parameters with the braiding and filament winding design parameters for desired complex shape geometry as developed in this work.

APPENDIX

A.1 Mathematical formulation of determining fiber angle using Netting Analysis

A circular cross-sectional structure with variable radius along its length, $r(z)$ under internal pressure and axial loading is considered here for the analysis.

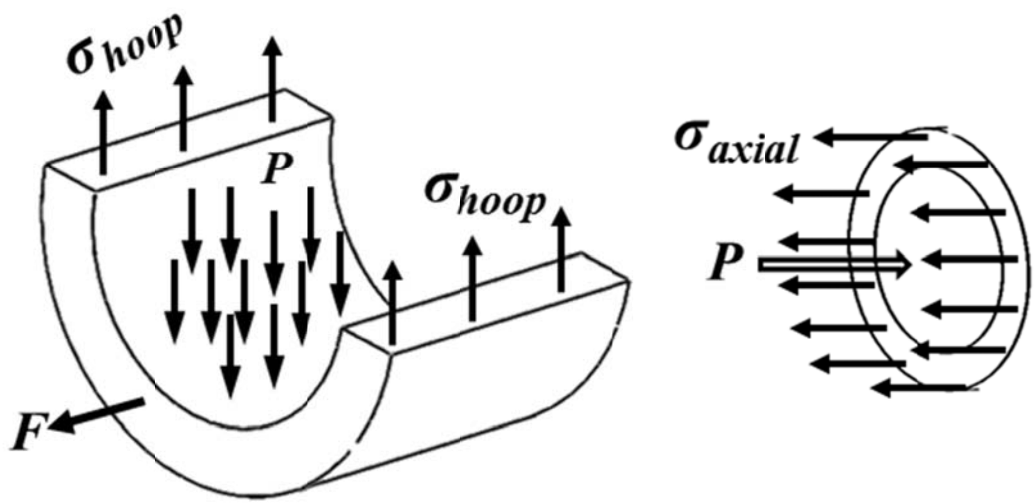

(a) (b)

Figure A.1: (a) Hoop stress and (b) Axial stress developed in the mandrel cross-section due to internal pressure and axial loading.

Equations of equilibrium for the internal forces caused by internal pressure and axial traction are developed. Therefore force balance considering the mandrel cross-section should be established.

Force in hoop direction due to pressure p,

$$\begin{aligned} F_h &= p \times Area \\ &= p \times L \times d \\ &= p \times L \times 2 \times r(z) \end{aligned} \tag{1}$$

Force induced due to hoop stress,

$$\begin{aligned} F_h &= \sigma_{hoop} \times Area \\ &= \sigma_{hoop} \times 2 \times L \times t \end{aligned} \tag{2}$$

Force in axial direction due to pressure p and axial load F,

$$\begin{aligned} F_a &= p * Area + F \\ &= p \times \pi r^2 + F \end{aligned} \tag{3}$$

Force induced due to axial stress,

$$\begin{aligned} F_a &= \sigma_{axial} * Area \\ &= \sigma_{axial} \times 2 \times \pi \times r \times t \end{aligned} \tag{4}$$

The cross sectional area per unit length of a strand along the layup direction shall be denoted as A_α (i.e. A_α has a dimension of length). The strand area along the hoop and axial directions per unit length are therefore $A_h = A_\alpha \sin\alpha$ and $A_a = A_\alpha \cos\alpha$, respectively. The force components per unit length in the hoop direction can respectively be resolved as:

$$F_h = \sigma_\alpha A_\alpha \sin^2 \alpha \tag{5}$$

$$F_a = \sigma_\alpha A_\alpha \cos^2 \alpha \tag{6}$$

Force in hoop and axial directions for the fiber oriented at ± α direction (valid according to the model assumptions using netting analysis described in section 3.3),

$$F_h = 2 \times \sigma_\alpha A_\alpha \sin^2 \alpha \tag{7}$$

$$F_a = 2 \times \sigma_\alpha A_\alpha \cos^2 \alpha \tag{8}$$

Using Eqs. (1), (2), and (7)

$$p \times L \times 2 \times r(z) \; = \sigma_{hoop} \times 2 \times L \times t \; = 2 \times \sigma_\alpha A_\alpha \sin^2 \alpha$$

i.e. from Eqs. (1) and (7),

$$p \times L \times 2 \times r(z) \; = 2 \times \sigma_\alpha A_\alpha \sin^2 \alpha$$

Or, $$p \times r(z) = \sigma_a \; A_a \sin^2 \alpha \qquad \text{[for unit length L=1]} \tag{9}$$

From (2) and (7),

$$\sigma_{hoop} \times 2 \times L \times t \; = 2 \times \sigma_\alpha A_\alpha \sin^2 \alpha$$

Or, $$\sigma_{hoop} * A = \sigma_a \; A_a \sin^2 \alpha \qquad [\text{where } A = L*t, \text{ when } L=1, A=t] \tag{10}$$

From (9) and (10),

$$p \times r(z) = \sigma_a \; A_a \sin^2 \alpha = \sigma_{hoop} * A \tag{11}$$

Similarly, using Eqs. (3), (4), and (8),

$$\frac{pr(z)}{2} + \frac{F}{2\pi\, r(z)} = \sigma_a\, A_a \cos^2 \alpha \tag{12}$$

$$= \sigma_{axial} * A$$

Dividing Eq. (11) by (12),

$$\frac{\sigma_{hoop}}{\sigma_{axial}} = \tan^2 \alpha = \frac{pr(z)}{\frac{pr(z)}{2} + \frac{F}{2\pi\, r(z)}} = \frac{2}{1 + \frac{1}{\pi\,(r(z))^2} \cdot \left(\frac{F}{p}\right)}$$

Or,

$$\alpha(z) = \arctan \sqrt{\frac{2}{1 + \frac{1}{\pi\,(r(z))^2} \cdot \left(\frac{F}{p}\right)}}$$